AD NUMBER

AD894806

NEW LIMITATION CHANGE

TO

Approved for public release, distribution unlimited

FROM

Distribution authorized to U.S. Gov't. agencies only; Test and Evaluation; SEP 1971. Other requests shall be referred to Plastics and Composites Branch, Nonmetallic Materials Division, Air Force Materials Laboratory, ATTN: AFML/LNC, Wright-Patterson AFB, OH 45433.

AUTHORITY

AFML ltr dtd 21 May 1973

AFML-TR-71-207
PART I

THE MODELING OF THERMOCHEMICAL ABLATION OF PYROLYZED PLASTICS AND GRAPHITES

PART I. APPLICATIONS OF OXIDATIVE THERMOGRAVIMETRY TO EVALUATING ARRHENIUS CONSTANTS AND DEFINING MECHANISMS

R. W. FARMER

TECHNICAL REPORT AFML-TR-71-207, PART I

FEBRUARY 1972

AIR FORCE MATERIALS LABORATORY
AIR FORCE SYSTEMS COMMAND
WRIGHT-PATTERSON AIR FORCE BASE, OHIO

NOTICE

When Government drawings, specifications, or other data are used for any purpose other than in connection with a definitely related Government procurement operation, the United States Government thereby incurs no responsibility nor any obligation whatsoever; and the fact that the government may have formulated, furnished, or in any way supplied the said drawings, specifications, or other data, is not to be regarded by implication or otherwise as in any manner licensing the holder or any other person or corporation, or conveying any rights or permission to manufacture, use, or sell any patented invention that may in any way be related thereto.

Copies of this report should not be returned unless return is required by security considerations, contractual obligations, or notice on a specific document.

AIR FORCE: 31-5-72/100

AFML-TR-71-207
PART I

THE MODELING OF THERMOCHEMICAL ABLATION OF PYROLYZED PLASTICS AND GRAPHITES

PART I. APPLICATIONS OF OXIDATIVE THERMOGRAVIMETRY TO EVALUATING ARRHENIUS CONSTANTS AND DEFINING MECHANISMS

R. W. FARMER

FOREWORD

This report was prepared by the Thermally Protective Plastics and Composites Section, Plastics and Composites Branch, and was initiated under Project 7340, "Nonmetallic Composites and Materials," Task 734001, "Thermally Protective Plastics and Composites." The work was administered under the direction of the Nonmetallic Materials Division, Air Force Materials Laboratory, with Mr. R. W. Farmer (AFML/LNC) as the Project Engineer.

This report was submitted by the author in September 1971.

Many of the items described in this report were commercial items that were not developed or manufactured to meet any Government specification, to withstand the tests to which they were subjected, or to function as applied during this study. Any failure to meet the objectives of this study is no reflection upon any of the commercial items discussed herein or upon any manufacturer.

This technical report has been reviewed and is approved.

T. J. REINHART, JR.
Acting Chief, Plastics and
Composites Branch
Nonmetallic Materials Division
Air Force Materials Laboratory

ABSTRACT

Future reentry vehicles will use pyrolyzed plastics and monolithic graphites for shape stable, thermal protection systems. Oxidation kinetic models and kinetic constants for these models will be necessary to predict (1) linear and mass losses, (2) altered heat and mass transport features of the ablation contaminated flow field, (3) the effects of ablative and contaminant species on optical/radar observables, and (4) related phenomena.

Constant heating rate thermogravimetry was used to study the fundamental kinetics and mechanisms of surface oxidation at temperatures to 1000°C. The materials included an ablative pyrolyzed plastic, an ammonium chloride-filled version of this material, three graphites, graphite fabric, and a carbon.

The thermograms of powder samples of the pyrolyzed plastic and most of the other materials were similar. Oxidative resistance was reduced by an increase in airflow rate, heating rate, oxygen concentration, pressure, or surface area. These sample and environmental responses were consistent with an Arrhenius-type kinetic model.

There was evidence of diffusive effects, of the type normally found at temperatures above 1000°C, in some of the heating rate, oxygen concentration, and surface area experiments. This unexpected result was tentatively explained in terms of a phase boundary control theory of surface oxidation.

The recording thermobalance was unsatisfactory in operation over a sufficiently wide range of sample and environmental variables for a comprehensive investigation of kinetics and mechanisms. A prototype version of a unique gas purge/vacuum network was therefore built and demonstrated over an extremely wide range of environmental variables.

TABLE OF CONTENTS

TABLE OF CONTENTS (CONTINUE)

ILLUSTRATIONS

ILLUSTRATIONS (CONTINUE)

SYMBOLS

SYMBOL	DEFINITION	SYMBOL UNITS
A	empirical Arrhenius constant*	$gm/atm^{1/2}\text{-}cm^2\text{-}min$
B	functional symbol	1/min
CT	crucible thermocouple temperature	°C
E	empirical Arrhenius constant	Kcal/gm-mole
ln ( )	logarithm to the base e	dimensionless
$\log_{10}( )$	logarithm to the base 10	dimensionless
$\dot{m}$	mass transfer rate	$lbs/ft^2\text{-}sec$
n	empirical order	dimensionless
P	pressure	atm
p(X)	$X^{-1} e^{-X} - \int_X^{\infty} X^{-1} e^{-X} dX$	dimensionless
r	$X^2 e^X p(X)$	dimensionless
R	gas constant	Kcal/gm-mole/°K
R_B	nose radius	feet
RT	reference thermocouple temperature	°C
S	surface area	cm^2
ST	sample thermocouple temperature	°C
t	time	min
T	temperature, degrees absolute*	°K
$\dot{T}$	heating rate, dT/dt	°K/min
w	fractional residual weight	dimensionless
w_o	residual weight	gm
X	E/RT	dimensionless

SYMBOL	DEFINITION	SYMBOL UNITS
z	oxygen mole fraction	dimensionless
Z	altitude	K ft
Subscripts		
c	corrected value	
e	outer edge of boundary layer	
l	isothermal value	
w	wall value	

*Different units for a symbol are noted with that symbol.

SECTION I

INTRODUCTION

Pyrolyzed plastics and graphites are capable of excellent ablative performance in severe hyperthermal environments. The low recession rates result from efficient heat rejection and a tolerance for pressure and shear mechanical effects. These materials are finding current use and are being further developed for such Air Force applications as heat shields, leading edges, nose caps, and rocket nozzles.

Oxidation is a major process in the ablation of pyrolyzed plastics and graphites. Oxidation consists of chemical, heat transfer, and mass transfer elements dependent upon surface temperature. Surface oxidation dominates up to about 2000°R. The surrounding, local oxygen is rapidly consumed at higher temperatures. Diffusion and associate gas-to-surface effects then control the overall rate of oxidation. Transition between surface and external control is a third rate-controlling region. Sublimation begins at very nigh temperatures and ultimately exceeds oxidative rates, thus controlling mass transfer.

Oxidation on the surface during graphite ablation is frequently expressed as

$$\dot{m} = A(zP_e)^n e^{-E/RT} \qquad (1)$$

where $\dot{m}$ is the mass transfer rate (as lbs/ft^2-sec) away from the surface, A is the first Arrhenius constant, z the mole fraction of surface oxygen,

P_e the static pressure at the boundary-layer edge, n the effective oxygen concentration exponent, E the second Arrhenius constant, R the gas constant, and T the temperature (Reference 1).

The Arrhenius-type correlation was originally derived from a review of various kinetic correlations and isothermal thermogravimetric data for a wide variety of carbons and graphites (Reference 1). More accurate correlations for surface oxidation as well as correlations for the transition and diffusion regions have been largely based upon Equation 1.

The kinetic constants n, A, and E cannot be directly intrepreted as fundamental properties as density or specific heat. Their physical dependence upon the nature of the surface, thermal history, and other fugitive variables is similar to the surface-dependent character of emittance. Consistent with this analogy, the surface reaction rates show not only the expected large dependence upon temperature but, further, a dependence upon type of graphite and its surface through the values of n, A, and E. In the transition and diffusion rate-controlling regions, however, mass transfer becomes relatively independent of the graphite, its surface, and surface temperature but is dependent upon the rate of oxygen supply. The surface reaction rates then show an expected large dependence upon n, P_e and P_w, and z.

A recently postulated mechanism of graphite oxidation suggests that surface reactions <u>alone</u> may control oxidation at most temperatures (Reference 2). The theory of phase boundary control specifically excludes

transition and diffusion effects suggesting temperature-dependent surface reactions to the sublimation region for a constant partial pressure of surface oxygen.

The postulated phase boundary control mechanism raises serious questions about the validity of experimental methods to (1) establish specific kinetic models, (2) measure kinetic constants for these models, and (3) verify postulated mechanisms. The questions stem primarily from two attendant characteristics of phase boundary control. The first effect is a dependence of an "apparent" rate-controlling mechanism upon critical sample and environmental variables that can affect the terms of Equation 1. Specifically, these variables could conceivably include airflow rate and the attendant influence upon local external and local surface oxygen concentration and pressure, static oxygen concentration and pressure, and surface area of the sample. The second effect is a shift in the effective temperature range of the apparent mechanism with a change in the magnitude of one of the variables. The important end result of these two effects is an incorrect value of n, A, or E.

In this report, several aspects of the surface oxidation of ablative pyrolyzed plastics and graphites are considered. A previous, constant heating rate, thermogravimetric study was first re-investigated in terms of better definition of kinetic models and mechanisms, with particular emphasis on phase boundary control. The responses of a variety of materials are discussed in fundamental terms. The effects of changes in sample and environmental variables found in some runs are explained in terms of a derived kinetic model for a constant heating rate.

There was evidence of diffusive effects in some of the oxygen concentration and surface area experiments that suggested transitional or diffusion control at far below normal temperatures. By postulating a phase boundary control-type mechanism, a method was then derived to identify the effective temperature range of true surface reaction control by assuming a step change in E or A, or a change in any other sample and environmental variable.

The relatively easy perturbation of an individual sample or environmental variable in constant heating rate thermogravimetry with the direct portrayal of the effective temperature range of the corresponding shift in the apparent mechanism was postulated to be a powerful tool for the study of phase boundary control effects.

An apparatus capable of operation over a wide range of constant values of airflow rate, heating rate, oxygen concentration, pressure, and sample surface area was shown to be essential for this type of study. To show that this extremely stringent requirement could be practically met (with the exception of sample surface area), a prototype gas purge/vacuum network was constructed and demonstrated to be compatible with the recording thermobalance.

The report concludes with detailed recommendations for apparatus arrangements, analytical methods, experimental methods, and sample configurations for the comprehensive study of surface oxidation kinetics and mechanisms using either isothermal or constant heating rate thermogravimetry. The historical use of thermogravimetric results to produce basic

numbers or to complement other techniques as ablation in an air arc heater, chromatography, effluent gas analysis, mass spectrometry, etc., justifies the continuing use of these methods. It is particularly believed that constant heating rate thermogravimetry can be a highly effective tool in a fundamental study of the phase boundary control theory of oxidation.

The importance of precision information on surface oxidation kinetics and mechanisms for a practical case of entry of a ballistic vehicle is briefly discussed in the following background section. Surface oxidation is shown to exist primarily at high altitudes and to result in little actual mass transfer. The mass loss is, however, potentially significant in terms of the production of electrons from contaminants present in the ablator. The background is concluded with projected needs for precision information from the end-use viewpoint of the prediction of high altitude optical/radar observables and related phenomena.

SECTION II

BACKGROUND FOR GRAPHITE ABLATION

An oxidative thermogravimetry experiment is relatively simple from external appearances. It is difficult to fully appreciate the highly complex heat transfer, mass transfer, and physicochemical processes that transpire. It is further difficult to comprehend how information from a thermogravimetry experiment may apply to the even more complex situation of ablation for a ballistic entry vehicle. This section gives a very brief introduction to important graphite ablation mechanisms, surface reaction kinetics, reaction products, high altitude aerothermochemical phenomena, and kinetic and observable dependencies upon graphite type. The general observations are considered to partially apply for high quality grades of pyrolyzed plastics in lieu of more definitive information. The background concludes with projected needs for kinetic models and kinetic constants for advanced ablative pyrolyzed plastics and graphites from an end-use viewpoint.

1. RATE-CONTROLLING MECHANISMS

Four fundamental mechanisms exist in graphite ablation. Oxidation begins on the surface at a relatively low temperature. The rate increases rapidly with increasing temperature. With the resulting depletion of local oxygen, the rate of diffusive supply across the boundary layer is eventually rate controlling. Combined diffusion, boundary layer composition, and surface reaction effects exist for an intermediate, transition case. At higher temperatures, sublimation begins and ultimately controls mass transfer (Reference 2).

There is a strong temperature dependence for the reaction, transition, and sublimation regions. Figure 1 illustrates mass transfer, normalized against the diffusion mass transfer, as a function of temperature (Reference 3). For the case of "fast" surface kinetics, the onset of reaction-, diffusion-, and sublimation-control occurs at about 1760, 2460, and 5960°R. Mass transfer dependence upon pressure is further shown by this parametric plot

2. SURFACE REACTION KINETICS

An Arrhenius correlation for surface reaction kinetics during ablation is

$$\dot{m} = A(zP_e)^n \exp(-E/RT) \qquad (1$$

The correlation was derived using numerous thermogravimetric data for many carbonaceous and graphitic materials together with basic fluid mechanics (Reference 2). The values of n, A, and E were dependent upon the study reviewed, the specific material, and the specific material sample. The ranges were: n = 0 to 2, E = 8 to 60 Kcal/mole, and A = 1 to 10^9 $lb/ft^2\text{-}sec\text{-}atm^n$. Two sets of A and E were selected for two limiting cases of "slow" and "fast" kinetics. The parameter n was taken as one-half.

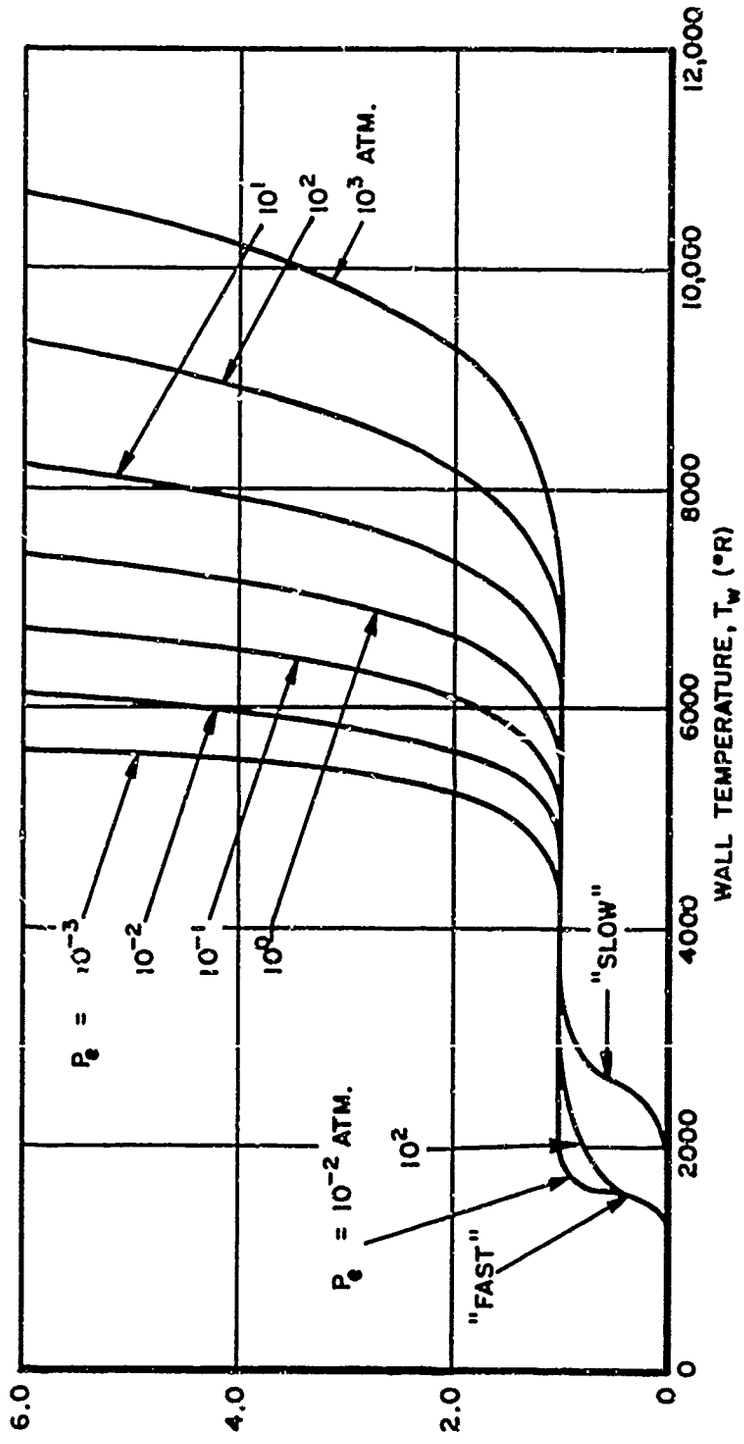

Figure 1. Fractional Mass Transfer Rates for Graphite Ablation as a Function of Stagnation Pressure and Wall Temperature

3. REACTION PRODUCTS

The primary reaction products are CO, CO_2, O, and O_2. Their spatial and temperature dependency were well illustrated by a recent rate-coupling similarity analysis for chemical equilibrium, a laminar boundary-layer, and a stagnation point (Reference 4). Flight conditions were for a 20 Kfps entry at 100 Kft.

CO_2 was found to dominate at the lower wall temperature and CO was most plentiful at the higher temperatures. At intermediate temperatures, the gas-solid products were coupled by multicomponent diffusion to the gas-phase products. There were limiting plateaus for mass transfer, as normalized with the one-half power of the ratio of the nose radius and the stagnation pressure at the boundary-layer edge (Figure 2). For "slow" kinetics, the plateaus resulted from O_2, CO_2, and CO domination below 2500, at 2500 to 3800, and above 3800°R, respectively. There were orders-of-magnitude change in near surface species with small changes in temperature. Modified "slow," or "slower" kinetics for an analysis using a different numerical method and property inputs gave an intermediate plateau somewhat displaced in position (Reference 5). Another analysis that approximated diffusion coupling agreed well at the lower temperatures, did not show intermediate plateaus, and predicted less mass transfer for the final CO asymptote (Figure 1, Reference 2).

The rapidly increasing rate of mass transfer with temperature at low temperature along with release of CO_2 was a strong function of surface reaction kinetics. The number of CO and CO_2 plateaus at intermediate

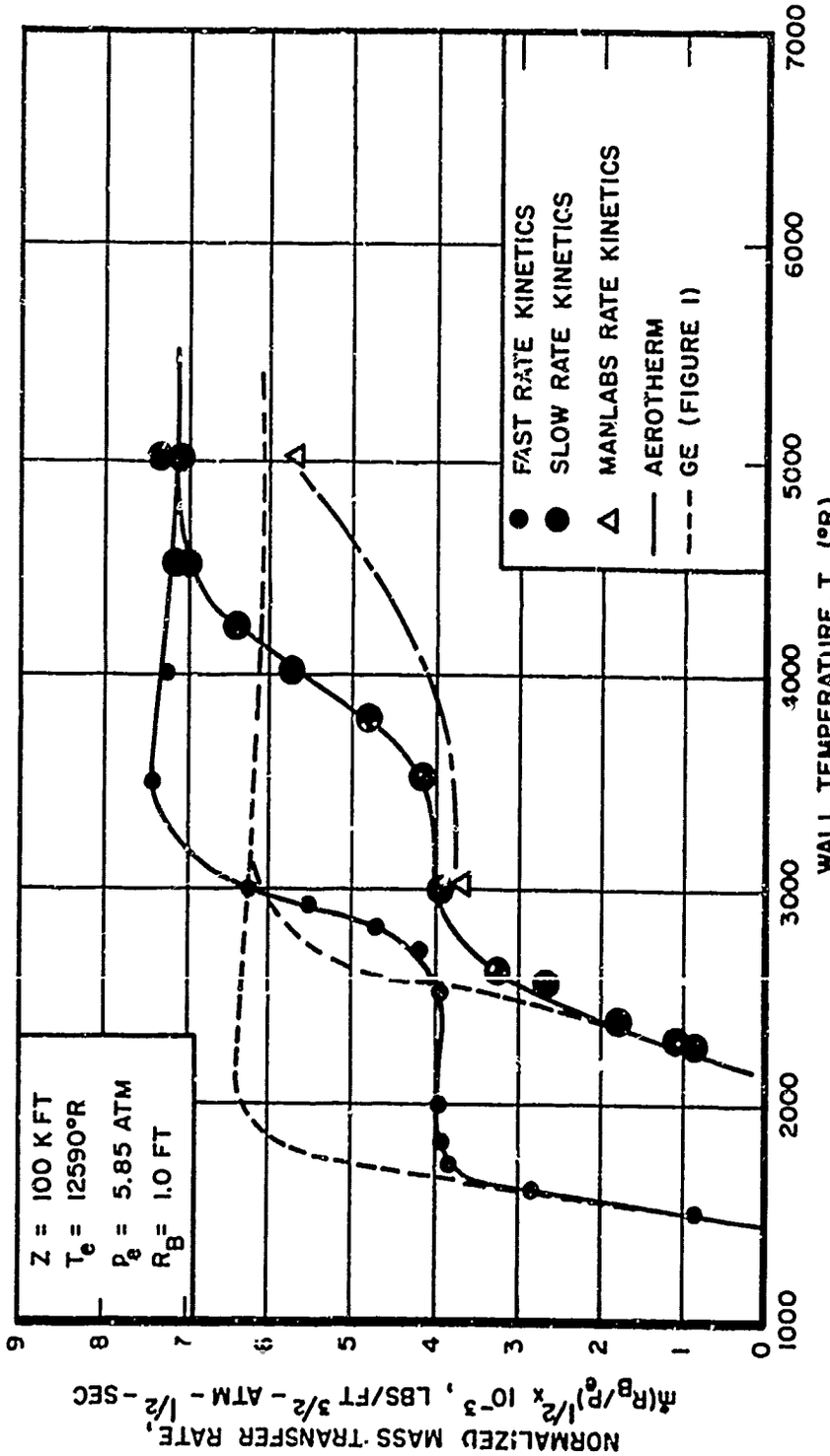

Figure 2. Normalized Mass Transfer Rates for Low Temperature Graphite Ablation

temperatures primarily involved chemical equilibria control of gas-phase composition and diffusion effects. The plateau characteristics were further dependent upon the magnitude of the kinetic constants.

4. EVALUATION OF ARRHENIUS CONSTANTS

Kinetic models and kinetic constants have been provided by a variety of analytical and experimental methods for numerous carbonaceous and graphitic materials. Typical results of a thermogravimetric study in air at atmospheric pressure for several graphites are summarized in Figure 3 (Reference 6). The large differences in oxidation rate at low temperature were markedly suppressed to a similar and higher rate at a higher temperature where diffusion effects were important.

Many isothermal thermogravimetric studies have been made in air, oxygen, and other gases at both high and low pressures over wide temperature ranges. Relative mass transfer rates calculated from models and constants for five graphitic investigations on different graphites are summarized in Figure 4 (Reference 2). A wide disparity is shown in any mass transfer rates predicted a priori from these results.

Two sets of kinetic constants were further verified indirectly in air arc heater experiments (Figure 5, Reference 7). The two sets corresponded to fast (as porous molded graphite) and slow (as pyrolytic graphite) kinetics. Flat-faced cylinders of ATJ graphite of three diameters were run in a hypersonic, low density airstream. A weighted averaging method was used to derive a universal kinetic model for surface reaction,

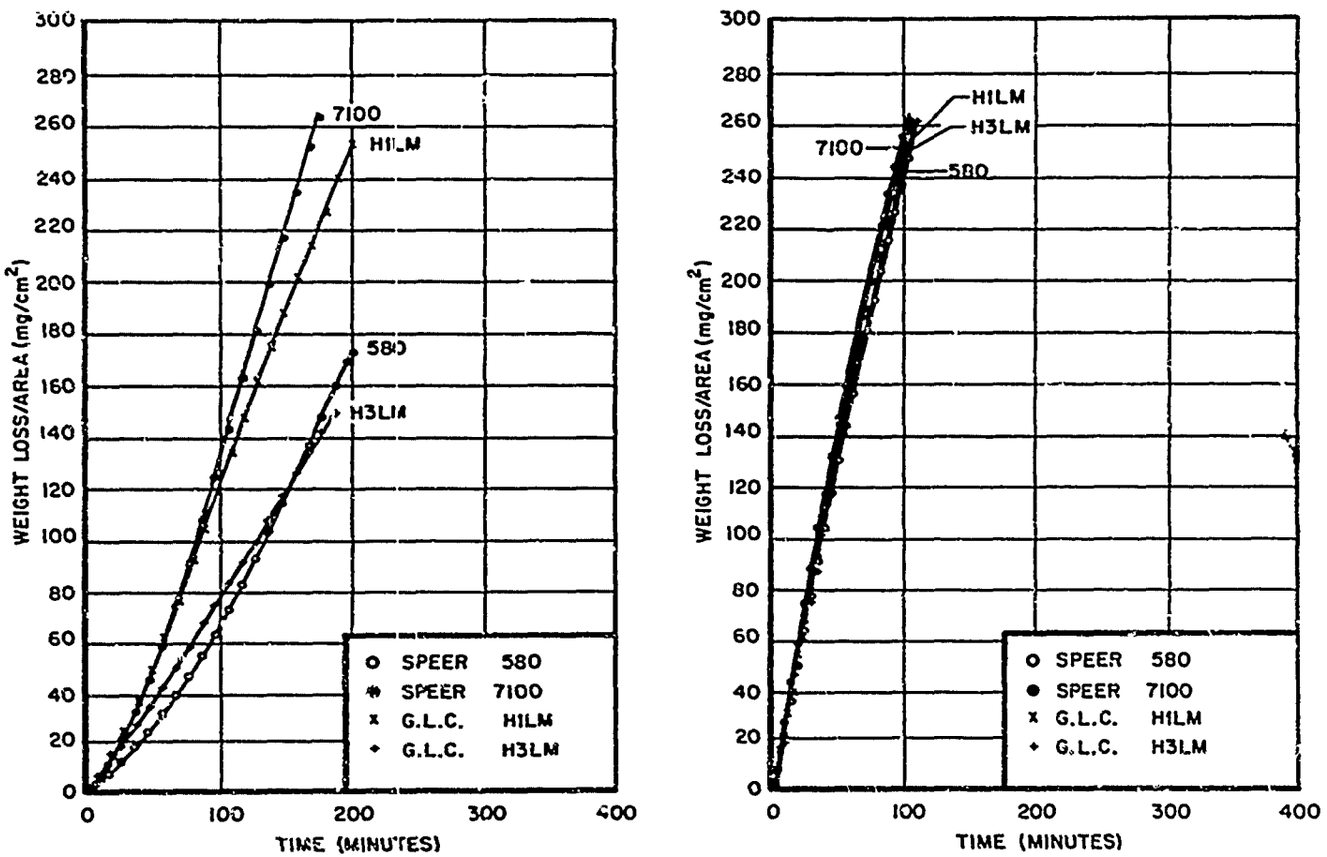

(a) Isothermal Temperature of 732°C (1350°F)

(b) Isothermal Temperature of 843°C (1550°F).

Figure 3. Temperature Effects on the Oxidation of Four Graphites

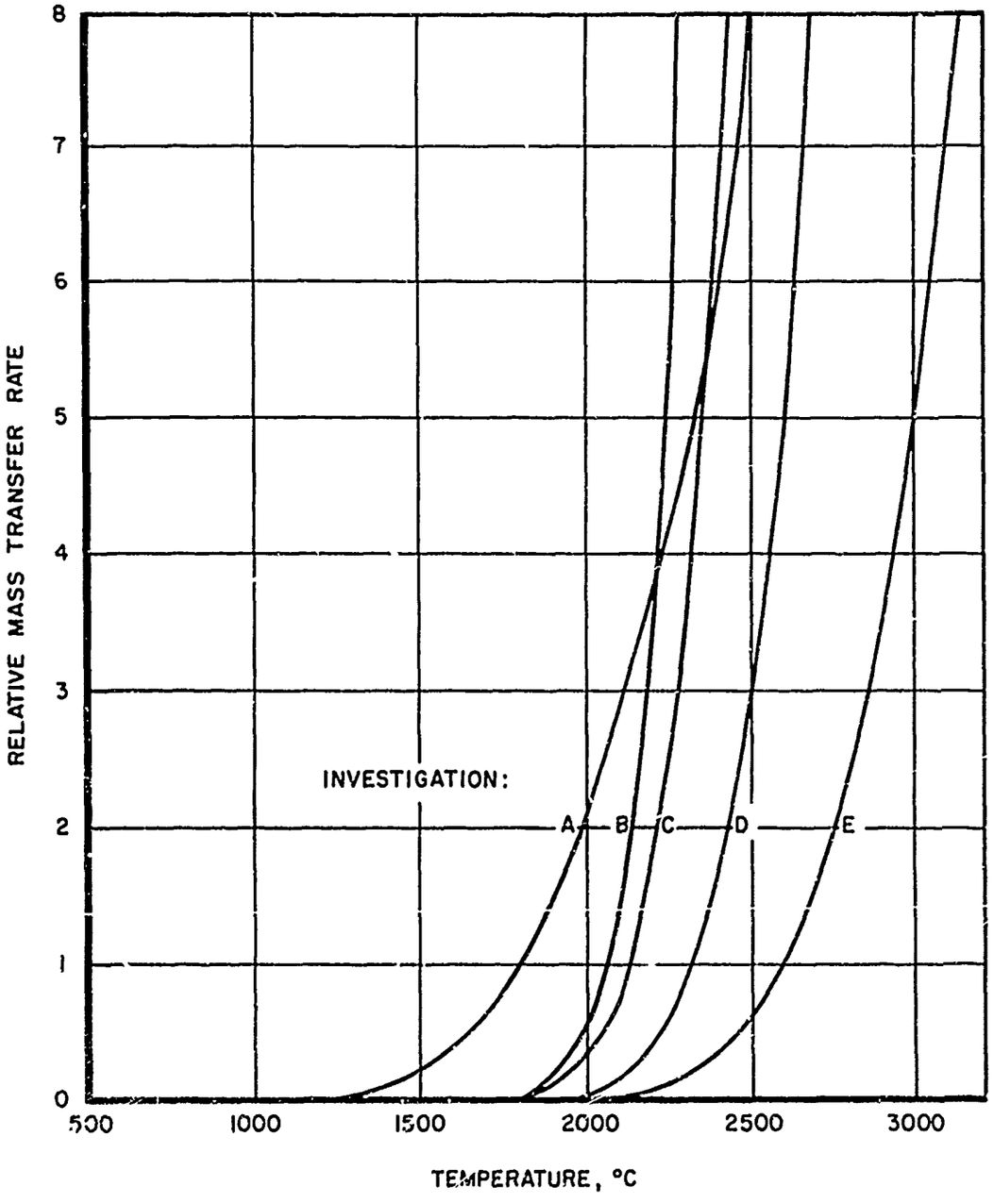

Figure 4. Potential Variation in Graphite Oxidation Due to Sample, Environment, and Kinetics Effects

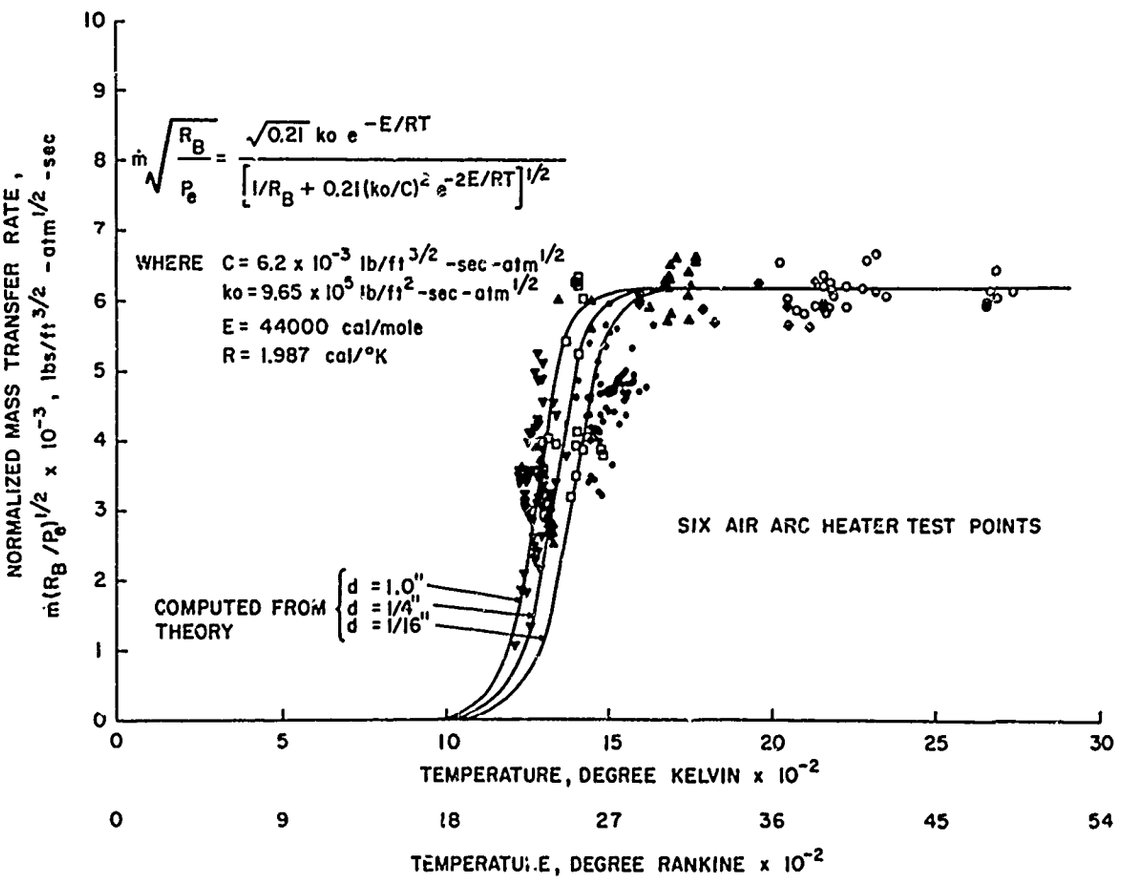

Figure 5. Normalized Mass Transfer Rates for ATJ Graphite Ablation

transition, and diffusion effects. Oxidation rates predicted by the model correlated, within some scatter, for surface temperatures from about 1300 to 2700°K (Figure 5).

Kinetics were investigated for three pyrolyzed plastics and two graphites using an air arc heater (Reference 8). Figure 6 illustrates a parametric plot for kinetic constants' evaluation. A comparison was made between mass transfer rates using the constants with rates for fast and slow kinetics based upon thermogravimetry as extrapolated by theoretical models to cover a wide temperature range (Figures 7 and 8). The pyrolyzed plastic and graphite mass transfer rates were effectively bracketed by the two calculated curves in the surface reaction region with individual mass transfer measurements agreeing well in the region of diffusion effects. There were, however, large differences at very high temperatures. The kinetic results were applied to aerothermochemical and thermostructural analyses for a hypersonic and a lifting vehicle entry mission.

A variety of experimental methods were applied in Reference 1 studies to investigate such principal variables as gas velocity, specimen configuration, temperature, and method of heating for a pyrolyzed plastic and five graphites. Figure 9 shows a temperature independent, oxidation limit due to inadequate oxygen supply for high velocity tests on inductively heated samples. The normalized values of oxidation were further compared with air arc heater results at three test points. Calculations were made to compare with numerous air arc heater runs of flat-faced samples with surface temperatures largely in the transition, diffusion effects, and sublimation regions. The calculations were based upon kinetic constants

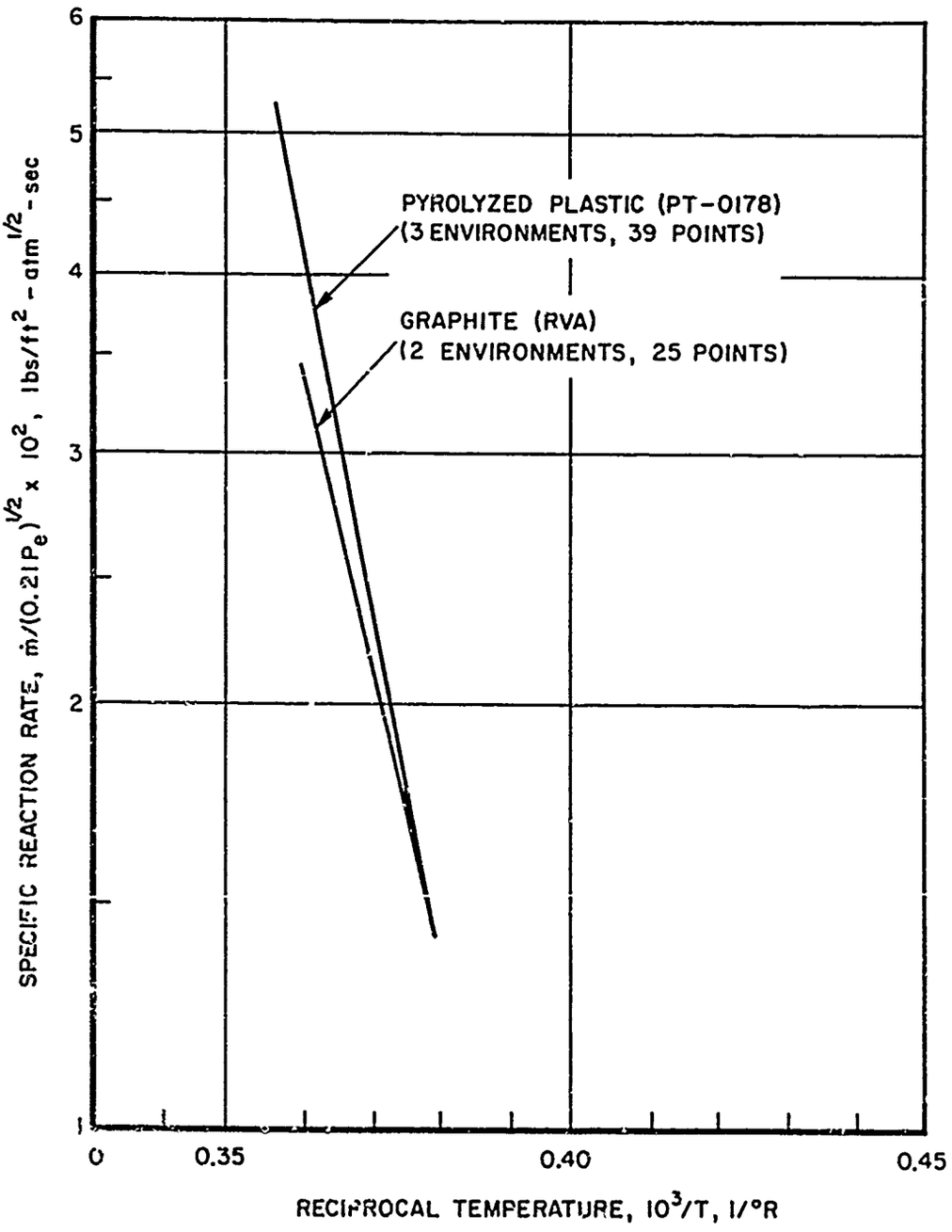

Figure 6. Arrhenius Plot for Pyrolyzed Piastic and Graphite Ablation

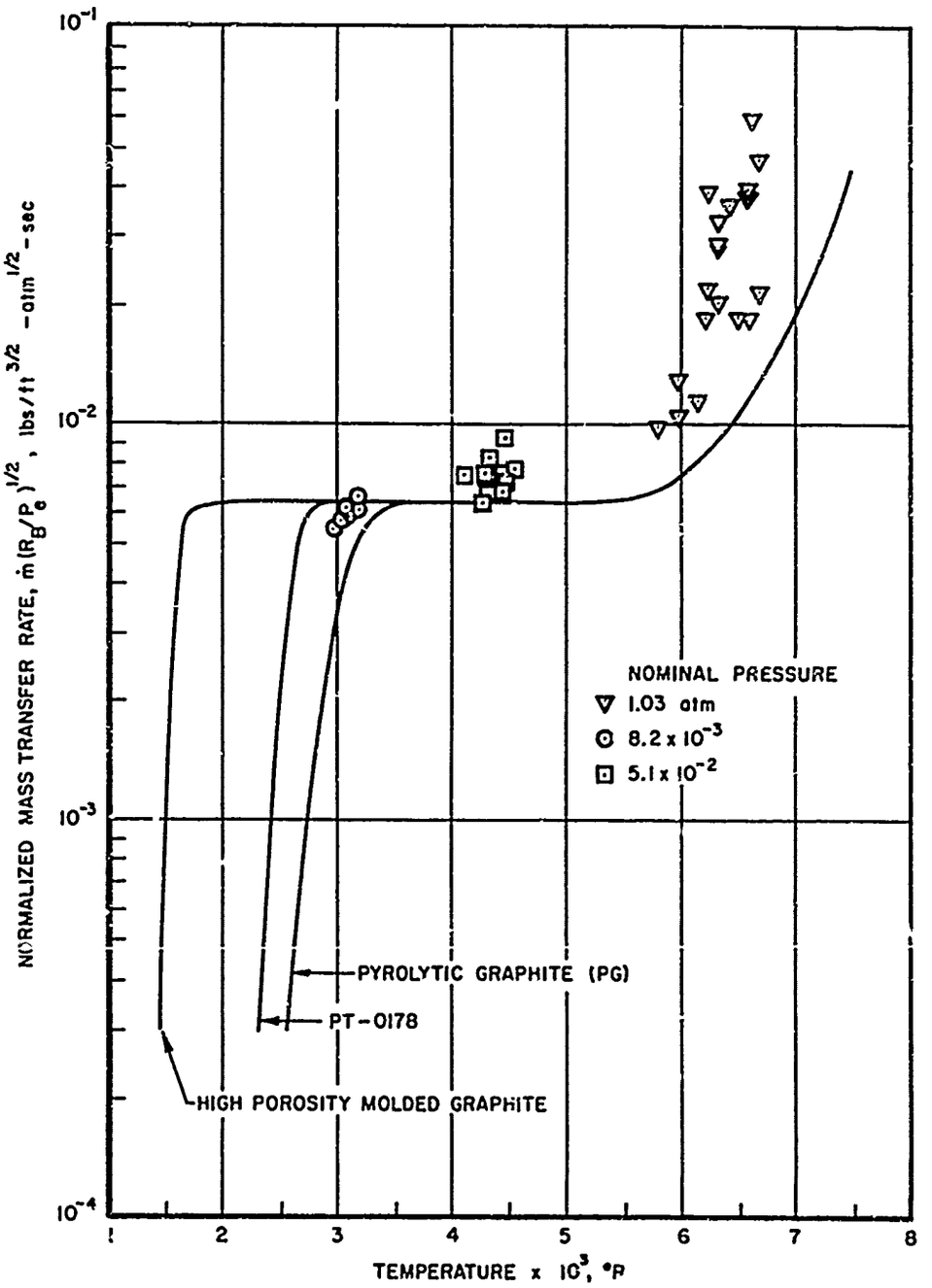

Figure 7. Normalized Mass Transfer Rate for PT-0178 Pyrolyzed Plastic Ablation

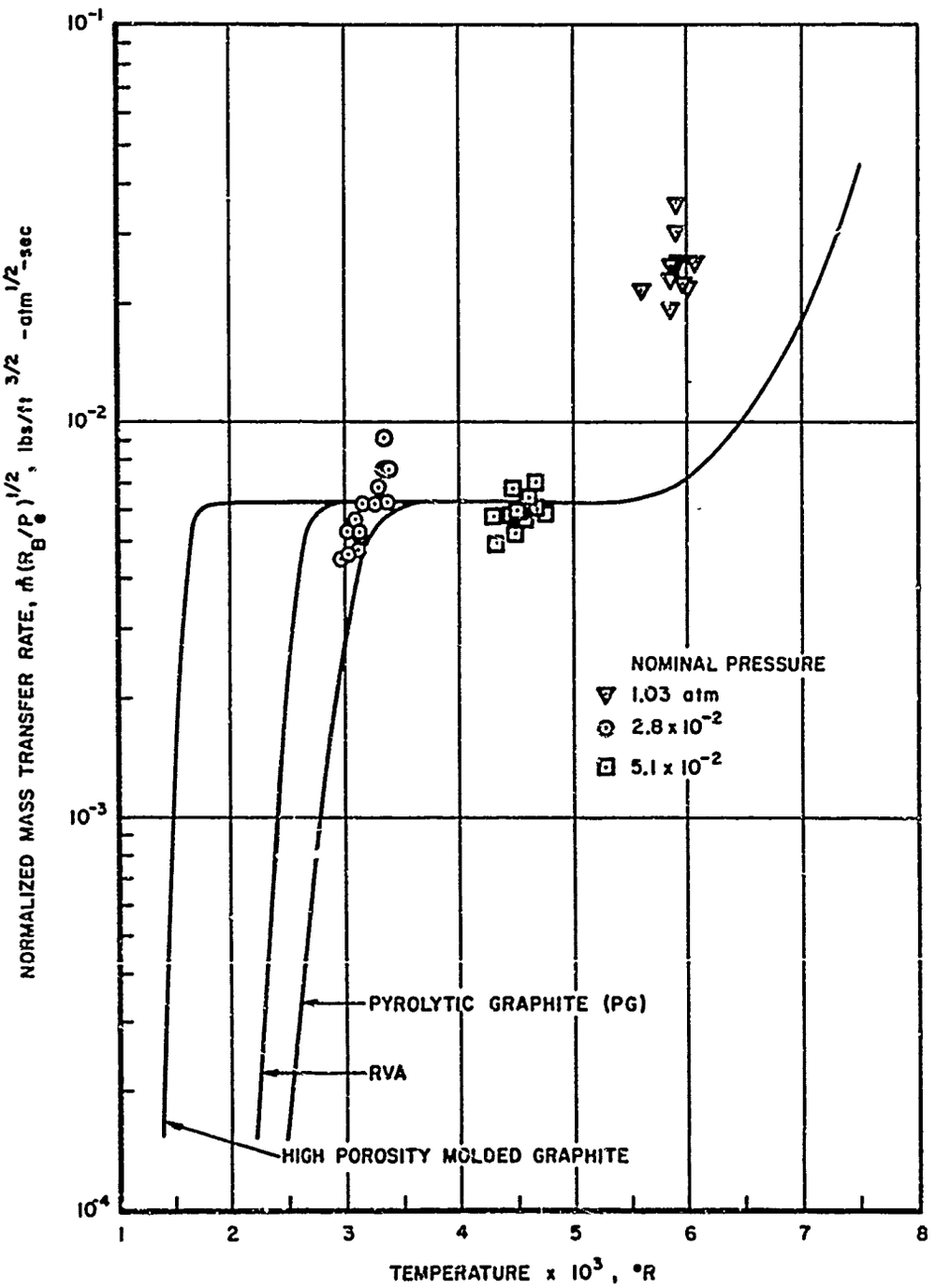

Figure 8. Normalized Mass Transfer Rate for RVA Graphite Ablation

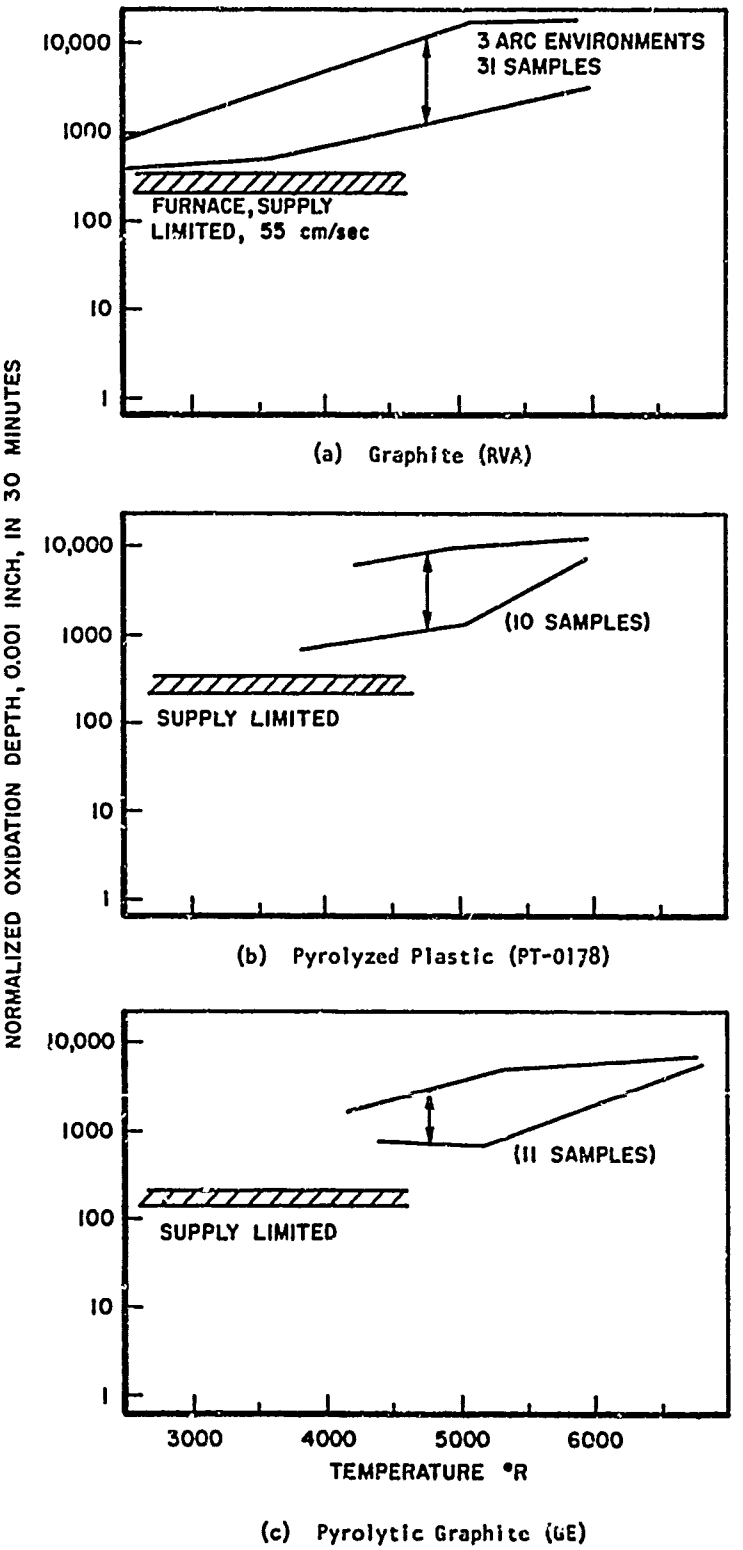

Figure 9. Air Arc Heater and Furnace Oxidation Depths for Various Materials

resulting from an examination of the laboratory experimental results to allow for airflow rates at subsonic velocities that were strikingly slower than for other values previously used in ablation analysis. The differences were tentatively attributed to CO_2/CO ratio influences partially affecting previous measurements.

The variations in the oxidation region over a wide range of pressures were studied for ATJ graphite using an air arc heater (Reference 9). The mass transfer results were adjusted to more properly reflect oxygen concentration at the ablating surface and a parametric plot was made to obtain Arrhenius constants (Figure 10).

Thermogravimetry was a contributing element in previous studies on the ablation of pyrolyzed plastics and graphites as illustrated by the few preceding examples. Typical values of n, A, and E were further selected for several previous investigations and are summarized as Table I. With some exceptions, the kinetic model is essentially that of Equation 1.

5. HIGH ALTITUDE ABLATION

Surface reaction and diffusion effects occur at high altitudes during ballistic entry. As a typical example, the altitudes for reaction, diffusion, and sublimation control onset are about 318, 306, and 150 Kft, respectively, for a 24 Kft/sec entry case (Reference 10). The corresponding surface temperatures are about 2000, 3000, and 5450°R for radiation equilibrium at the nose cap stagnation point (one foot radius).

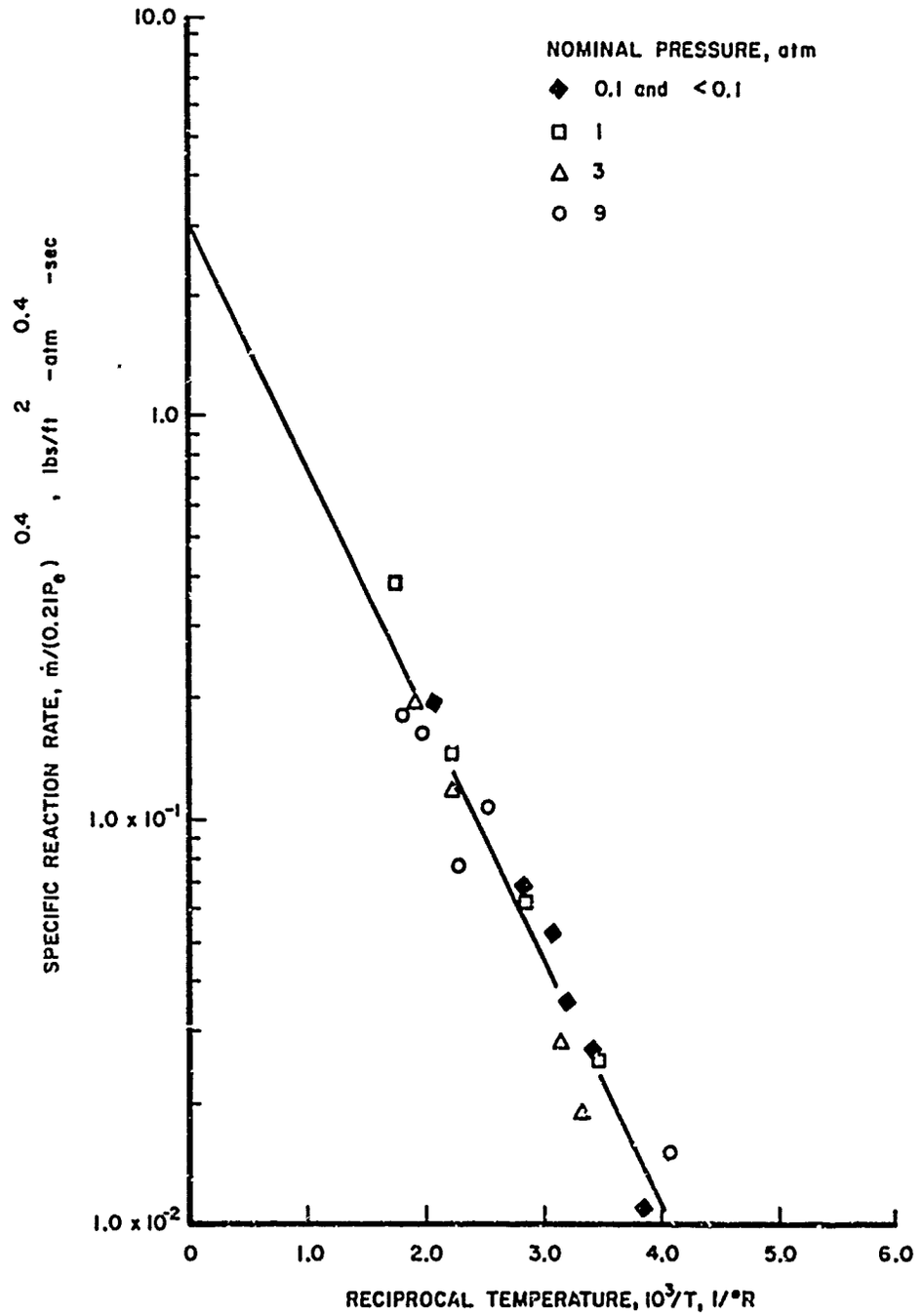

Figure 10. Arrhenius Plot for ATJ Graphite Ablation

TABLE I

REPRESENTATIVE KINETIC PARAMETERS FOR CARBONS, GRAPHITES, AND PYROLYZED PLASTICS

Material	n	E, KCal/ mole	A, lbs/ft^2-sec-atm^n	Method	Remarks	Reference
Carbons and Graphites						
ATJ	0.4	15.5	3.0	air arc heater	adjusted for oxygen at surface; Arrhenius plot	9
RVA	1/2	54.5	1.87×10^6	air arc heater	Arrhenius plot	8
RVA, Purified	1/2	27.3	$6.1/\times10^2$	air arc heater	Arrhenius plot	8
High Porosity Molded Graphite	1/2	44.0	6.73×10^8	thermogravimetry primarily	from literature review	8
ATJ, RVA, POCO	1/3	10.73	0.73	various tests		1
Various Carbons and Graphites						
Fast	1/2	44.0	6.73×10^8	thermogravimetry primarily	from literature review	2
Slow	1/2	42.3	4.47×10^4	thermogravimetry primarily	from literature review	2
Slower	1/3	9.0	0.532			5
Pyrolytic Graphite						
Optimistic	1/2	32.8	3.07			16
Conservative	1/2	47.5	1.28×10^4			16
Pyrolytic Graphite	1/2	47.5	1.28×10^4		for reference purposes	8
Pyrolyzed Plastics						
PT-0178	1/2	66.5	1.18×10^8	air arc heater	Arrhenius plot	8
PT-0181	1/2	25.5	1.69×10^2	air arc heater	Arrhenius plot	8
PT-0182	1/2	42.5	4.44×10^4	air arc heater	Arrhenius plot	8
PT-0178	1/3	10.73	0.73	various tests		1

High altitude optical/radar observables and other phenomena dependent upon specie distributions can be markedly affected by the release of ablative and, in particular, contaminant species. Alkali metals are easily ionized and release many electrons. In practice, the material metal level is usually proportioned to total mass transfer rate for initial calculations. As a highly approximate example for illustration, a factor of four change in metal injection rate could conceivably lead to a variation of three in mean electrons/cc and a large deviation of 10 dbsm in radar cross section (Reference 11).

6. FUTURE REQUIREMENTS

Commercial pyrolyzed plastics and graphites for candidate ablative use are contaminated by numerous elements and compounds. A first assessment was made for three graphites and a purified grade using manufacturers and other unpublished data. The detectable levels of three easily ionized alkali metals, in ppm, were in the nominal ranges of 0 to 90 for calcium, 3 to 11 for potassium, and 0 to 120 for sodium. The dominant impurity was calcium. The largest data scatter was also found for this element. With further review, few data could be found for pyrolyzed plastics. The contamination was expected to be relatively high, a result of a high concentration of impurities for the starting materials and many processing steps.

High accuracy kinetic models and kinetic constants will not necessarily be required for advanced ablative pyrolyzed plastics and graphites. The total mass loss is relatively small for the comparatively mild heating

and short times that surface reaction and diffusion mechanisms function for ballistic entry. Adequate kinetic information can probably be provided by the primary current method of air arc heater characterization and Arrhenius parametric plots.

Depending upon requirements, however, the analysis of high altitude optical/radar observables and related phenomena could dictate precision kinetic data. This is primarly due to (a) the strong dependence of mass transfer rate on temperature at low surface temperatures and (b) the large quantities of electrons that can be produced by minute quantities of contaminants from an impure ablative material. This preliminary study has suggested that improved analysis and experiments for specific ablative pyrolyzed plastics and graphites could be required for the prediction of impurity injection rates within factors of two to ten for surface reaction control at high altitudes.

This section emphasized a graphite nose tip and a pyrolyzed plastic heat shield for a ballistic entry vehicle. Diffusion effects, rather than sublimation, can dominate total mass loss in other types of entry (Reference 7). Precision kinetic models and kinetic constants, therefore, can be essential to analyses for certain areas of entry vehicles for hypersonic, lifting, low angle, and other cases.

SECTION III

EXPERIMENTAL MATERIALS

1. PYROLYZED PLASTICS

Two pyrolyzed plastics were tested; their preparations and properties have been described in Reference 12. A composite was first prepared from Union Carbide WCG graphite fabric and Coast Manufacturing Company R-120 phenolic resin. The composite was pyrolyzed in an inert atmosphere up to a maximum temperature of 815°C. A filled version of the pyrolyzed material was prepared by immersion into a boiling saturated solution of ammonium chloride. The residual ammonium chloride content was about 24% by weight.

The pyrolyzed plastics were machined into cylinders 3/4 inch in diameter by 1/2 inch in thickness. Fine powders were prepared for thermogravimetry by cryogenic grinding. A cylinder was first immersed into liquid nitrogen and pulverized with a carbide-tipped drill. The drill press speed was 1950 RPM. The powder was collected and manually sieved to pass a US Standard No. 325 screen.

Ammonium chloride powder was used for reference purposes. The coarse, commercial powder (reagent grade) was ground at room temperature with a mortar and pestle. The -100/+120 screen fraction was used for thermogravimetry.

2. GRAPHITES

The carbon and graphite materials were originally in a variety of configurations. The materials, all products of the Union Carbide Corporation, and original forms consisted of AGKSP electrode, ATJ electrode, WCB graphite fabric, Grade 40 porous carbon, and Grade 40 porous graphite in the form of flat panels.

The cryogenic method was used to prepare fine powders with the exception of WCB graphite fabric. This material was ground with a mortar and pestle. All powders were sieved to pass the 325 screen.

SECTION IV

THERMOGRAVIMETRY PROCEDURE

1. INTRODUCTION

Constant heating rate thermogravimetry is a dynamic version of the classical isothermal experiment. The weight/temperature thermogram is continuously generated by a recording thermobalance with temperature increasing at a fixed rate.

The oxidative thermogram of a pyrolyzed plastic or graphite is uniquely different from an isothermal counterpart. The thermogram is a kinetic history from solid to total gas. Differences existing between materials or sample constituents at only critical isothermal temperatures can often readily show within the wide range of temperature. The perturbations, as uncovered by many isothermal runs, of a single sample or environmental variable change can stand out in the constant rate thermogram.

Systematic changes in sample and environmental variables are possible in constant heating rate thermogravimetry. The thermogram can help quickly sort out the thermogravimetric result of these changes. The method was thus felt to be ultimately helpful, when applied with other suitable techniques, in elucidating complex kinetics and mechanisms.

2. RECORDING THERMOBALANCE

A modified Aminco Thermo-Grav recording thermobalance was used for constant heating rate thermogravimetry at 9°C/min to 950°C (Figure 11). This instrument and experimental procedures for its use have been previously described in detail (Reference 13). This report section gives a brief summary of relevant functions and methods.

The weight/temperature thermogram was automatically plotted by an X-Y recorder. During the run, sample weight change moved two precision springs. A linear variable differential transformer (LVDT) response drove the recorder pen. A Chromel alumel thermocouple gave the emf to move the X-axis carriage.

The balance components were enclosed within a Pyrex/quartz envelope. The suspension system included a top, two springs, a support rod with fixtures, and, at the far end, a crucible and holder. The Pyrex support rod was centrally joined to the springs. This rod held the LVDT core, a calibration weight in a tare pan, and an oil dashpot ring.

The Coors 230 3/0 crucible was made of porcelain. The furnace tube and integral thermocouple sheath were made from quartz. The 0.010 inch diameter thermocouple wires were insulated with ceramic spines and placed in the sheath in proximity to the sample crucible.

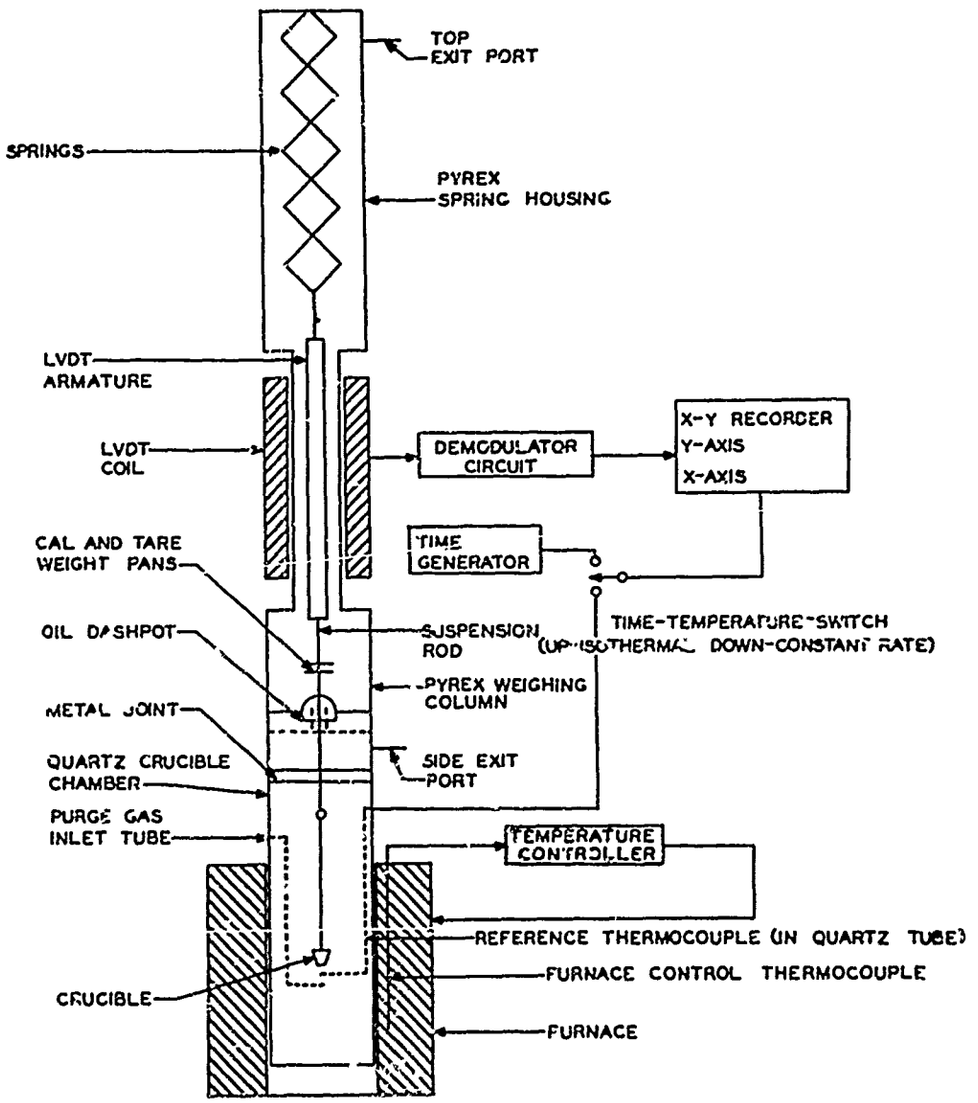

Figure 11. Thermo-Grav Functional Diagram

Heating rate was closely regulated by a furnace controller. The Chromel alumel thermocouple for the controller was located within the annular wall of the furnace.

3. EXPERIMENTAL METHODS

All powders were first "dried" at 100°C for 30 minutes in a small vacuum oven. The samples were then stored in a vacuum desiccator. A specific sample was removed and permitted to "equilibrate" at ambient room conditions prior to beginning a run.

The standard run was for a -325 screen, dried 100 mg powder at 9°C/min to 950°C in initially quiescent air. An analytical balance was used for weighing out the sample and weighing any run residue ($\pm$ 1 mg). There were a number of runs at other than standard conditions. The specific conditions were annotated on the respective thermogram.

SECTION V

DISCUSSION OF RESULTS

1. PYROLYZED PLASTICS

Air Force application areas for pyrolyzed plastics include heat shields and nose tips of entry vehicles. The low recession rate and fair insulative ability is a well known result of mass injection blockage, oxidative resistance, surface radiation, surface sublimation, and a relatively porous structure.

An experimental pyrolyzed plastic was made by inert atmosphere pyrolysis of a graphite fabric/phenolic resin composite to 815°C. This matrix was impregnated with ammonium chloride for internal endothermic decomposition, the release of large quantities of gas, and porosity reduction. Improved ablative cooling and efficient insulative ability were the primary goals

Ammonium chloride and other impregnants as ammonium fluoborate, tungsten diboride, etc., became of additional interest in later work in potentially altering high altitude optical/radar observables and related phenomena. Low impregnant concentrations could alter the rates of consumption and production of electrons and other flow field species. High concentrations could further alter flow field temperature and velocity distributions.

Thermograms for the pyrolyzed plastic, filled composite, and ammonium chloride were sketched together (Figure 12). The pyrolyzed plastic thermogram for air resembled an elongated arc tangent function. Weight loss began near 400°C. There was little sample left above 900°C. A major maximum rate of weight loss peaked near 530°C; a subdued peak was found around 700°C. This thermogram was similar to one for WCB graphite fabric. There was little weight loss for either material in vacuum. This implied efficient phenolic resin conversion into a carbonaceous material during pyrolysis.

The thermograms for the pyrolyzed plastic and ammonium chloride were essentially additive by a law of mixtures to give the filled composite result for both air and vacuum. Weight loss in vacuum was almost entirely due to the filler. There was a major and a minor maximum rate of weight loss peak for the filled composite in air near 400 and 700°C, respectively.

The ammonium chloride powder was more thermally stable in air than in vacuum. This result was consistent with normal vapor pressure relationships.

2. GRAPHITES

Air Force application areas for graphites include nose tips of entry vehicles. The high erosion resistance is a result of internal conduction and storage, mass injection blockage, oxidative resistance, surface radiation, and surface sublimation.

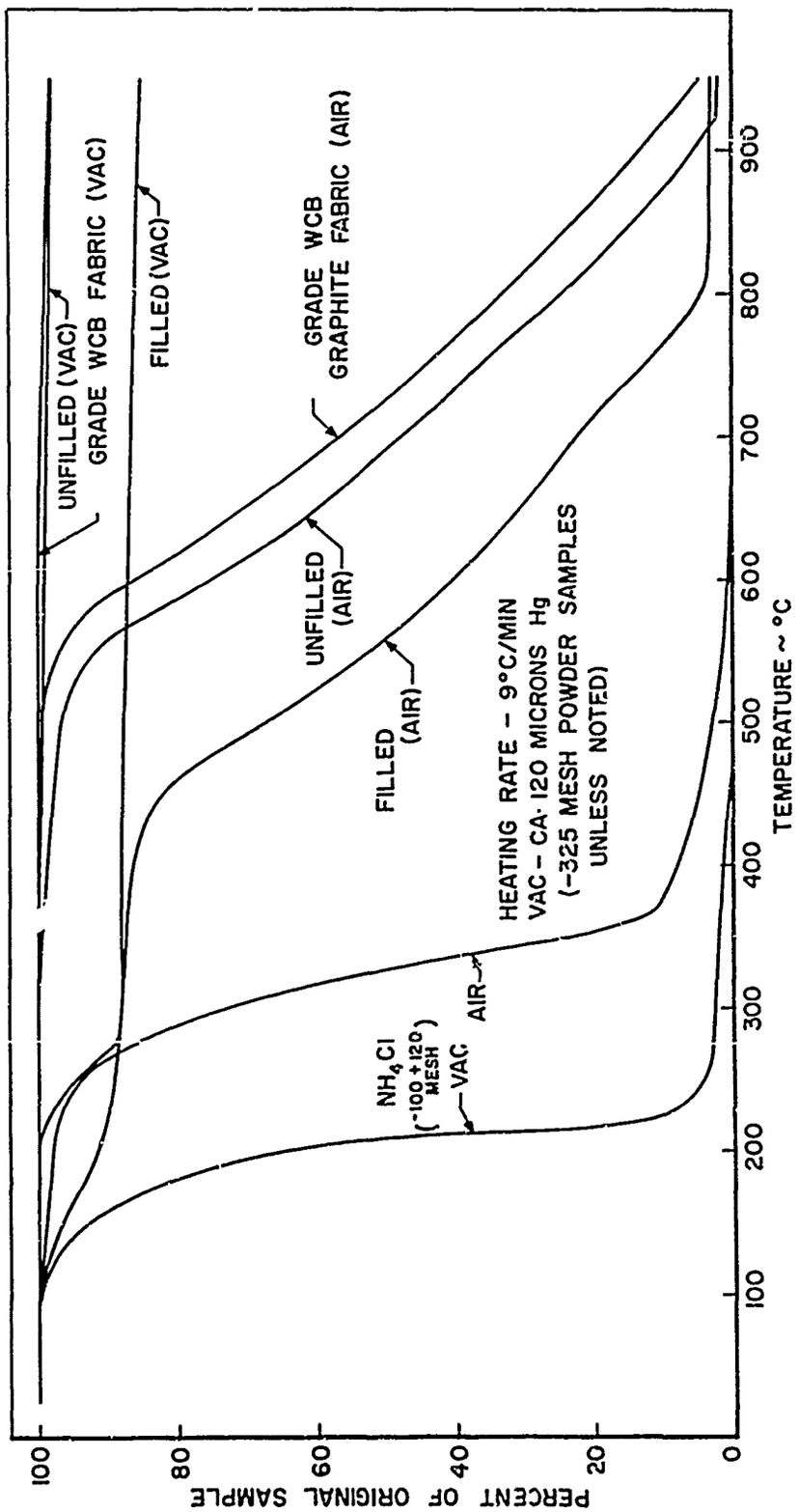

Figure 12. Thermograms for Pyrolyzed Plastic and Component Materials

The oxidative thermogravimetry of powders of four carbonaceous and graphitic materials gave similar results (Figure 13). The thermograms were for ATJ graphite, Grade 40 porous carbon, WCB graphite fabric, and the pyrolyzed plastic. Weight loss commenced near 525°C with little residue remaining above 950°C. There was an early maximum rate of weight loss region. A second maximum, suggested by thermogram shape, was never reached except for the pyrolyzed plastic.

The AGKSP graphite thermogram revealed relatively high oxidation resistance (Figure 13). This result was possibly associated with the high purity of this material, a small effective pore volume or surface area, or other unknown factors.

The presence of impurities can influence oxidation rates. For example, the oxidation susceptibility of carbon fabrics is well known to be highly sensitive to relative hydrogen activity. The effect of pH on the oxidation of two carbon fabrics is shown by Figure 14 (from Reference 14). The susceptibility was markedly reduced by an increase in pH, the primary impurity being sodium in the form of hydroxide. Large effects were also reported in further isothermal runs.

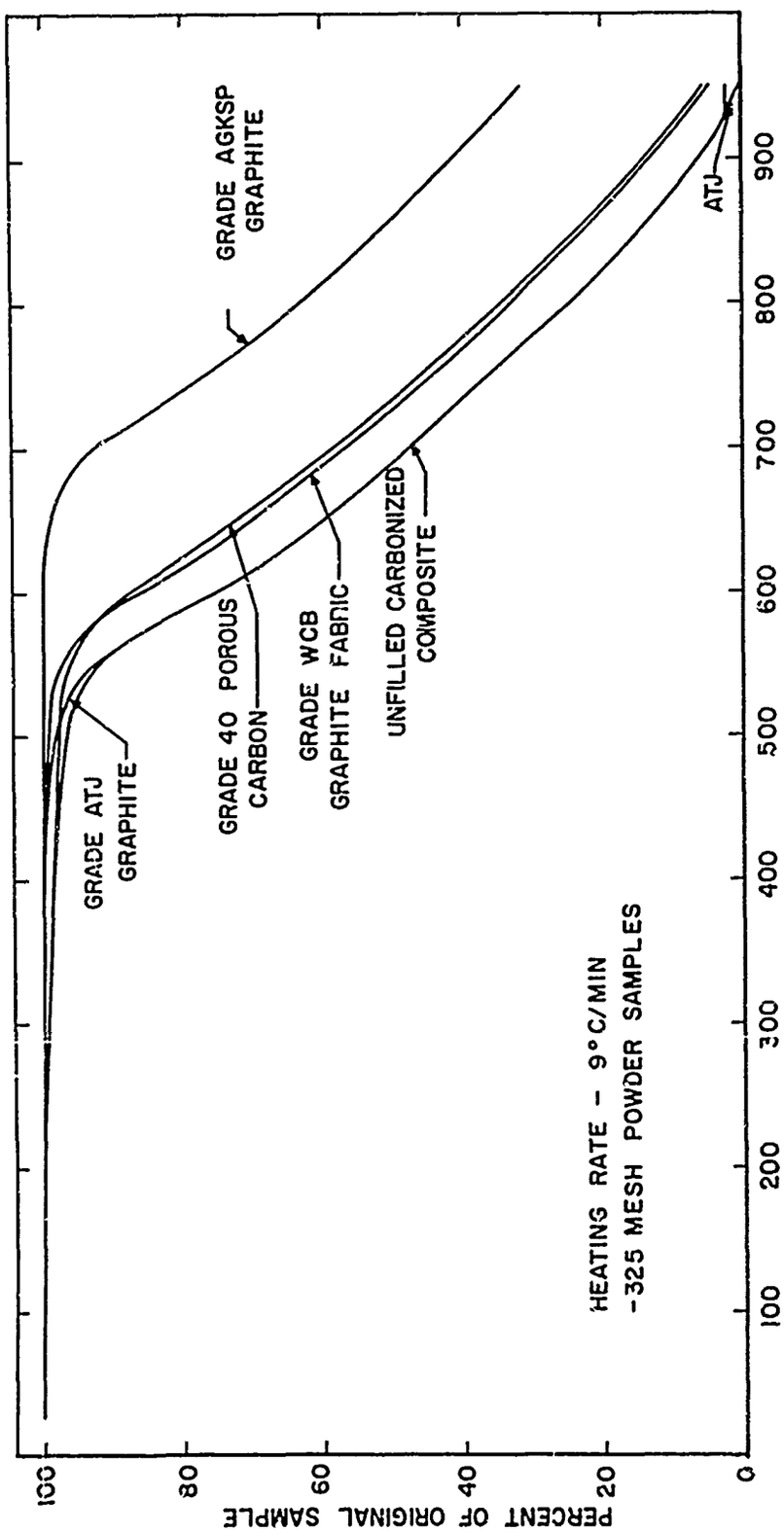

Figure 13. Thermograms for Carbonaceous and Graphitic Materials

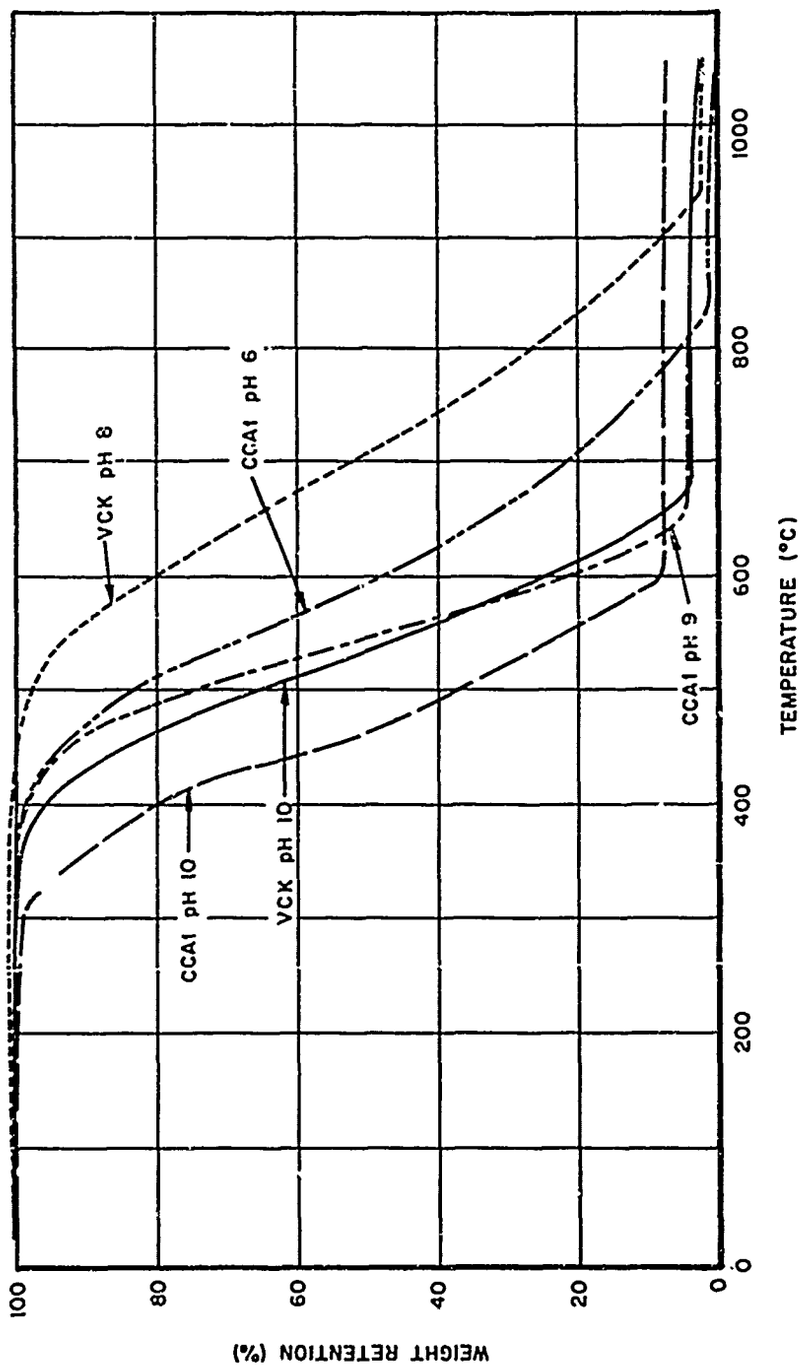

Figure 14. pH Effects for Two Carbon Fabrics

SECTION VI

KINETICS AND MECHANISMS OF GRAPHITE SURFACE OXIDATION

1. INTRODUCTION

The oxidation of carbon and graphite was a subject of analytical and experimental study over the past century. The classical processes, evolved primarily from heterogeneous mechanisms for carbon, coal, graphite, and coal models, considered surface reaction to control oxidation at low temperatures. Diffusion processes were the rate-controlling mechanism at higher temperatures. There was a complex transition intermediate between these two regions.

The specific surface reaction mechanisms have not been comprehensively identified and understood. It is generally accepted that the three basic processes are diffusion of gaseous reactants to a reactive surface site, physical reaction, and gaseous product desorption (Reference 2). There are many remaining questions as to the exact role of pores and regions between pores, the influence of catalytic agents and contaminants, the effects of absorbed water and other surface gases, surface activation, surface reactivity for specific graphite grades, surface chemical groups, etc. From a physical standpoint, oxidation for surface reaction control is considered to be highly dependent upon the specific nature of the graphite sample and its surface characteristics, relatively independent of the rate of oxygen supply (excluding total starvation), and extremely dependent upon temperature (Reference 2).

Oxygen consumption increases rapidly with temperature for active surface reaction processes. The surface region is depleted in oxygen and enriched in CO, CO_2, and N_2. The decrease in available oxygen reduces the rate of surface reaction. The transport of more oxygen, by normal or thermal diffusion, or other process, increases the oxidation rate. This low oxygen pressure at the surface leads through a transition intermediate to a steady-state transport balance between O_2 "in" and CO, CO_2, and N_2 "out."

True diffusion control is dependent upon the surroundings. Mass transport equilibrium results in an oxygen surface pressure below that of the surroundings. A perturbation of the system, as an increase in gas velocity, that changes the local pressure also changes the rate. An increase in surface temperature only will not result in a rate increase if local pressure is controlling the rate for a constant gas temperature. Therefore, these and more complex considerations result in the generally accepted viewpoint that true diffusion control is relatively independent of surface (not gas) temperature, strongly dependent upon the surroundings, and relatively independent of the type of graphite.

A more recent postulated mechanism for oxidation is phase boundary control. The review of Reference 1 suggests that surface reactions alone control oxidation and are temperature dependent to at least 6000°F (3340°C) for a constant partial pressure of surface oxygen. There is a low temperature region of CO_2 dominance with a high value of E (about 40 Kcal/mole), a moderate temperature region with rapid CO and CO_2 production corresponding to a low value of E (3-5 Kcal/mole), and a high temperature

region with CO as a primary product and an intermediate value of E (10-15 Kcal/mole). Phase boundary control is difficult to experimentally verify over diffusion control due to the strong system dependence of the latter. Reference 1 presents initial supporting evidence based upon extensive results on gas velocity, pressure, and temperature effects. In particular, an increase in velocity results in a "restoration" of rate dependance upon temperature. Rate dependence upon temperature is a major characteristic of surface reaction control. Further, the rate is shown to vary with local pressure to the 0.3-0.5 power, a potential result for phase boundary control.

An important conclusion for phase boundary control of graphite oxidation is that local pressure dependence and changes in E are closely tied to the translation from one oxidative region to another. An accurate characterization of the kinetic model, its pressure dependence, and kinetic constants is desirable in the prediction of graphite ablation over a wide range of pressure and temperature.

Kinetic models of graphite oxidation were proposed in numerous previous studies and experimental data were fitted to evaluate kinetic constants for these models. A basically different approach was taken in this preliminary study. A kinetic model with important sample and environmental terms was used to help interpret the results of the novel application of constant heating rate thermogravimetry. Other than maintaining sample and environmental variables at an initially constant level by procedural consistency, there was no intent or attempt to match ideal

requirements as necessary for factual kinetic constant evaluation. To use this approach, a brief analysis was necessary to convert the isothermal relation into a constant heating rate case.

2. KINETIC MODEL

The extensive review of surface reaction oxidation of a variety of carbons and graphites under Reference 2 resulted in the following Arrhenius correlation

$$-dw/dt = A(S(zP)^{n}/w_o)\, e^{-E/RT} \tag{2}$$

A term B was useful for "lumping" the variables of a single experiment, thus

$$B = A(S(zP)^{n}/w_o) \tag{3}$$

and gave the result

$$-dw/dt = B\, e^{-E/RT} \tag{4}$$

The isothermal solution of Equation 4 was simply

$$(1 - w_I) = Bt_I\, e^{-X_I} \tag{5}$$

for assumed reaction initiation at zero time. (The subscript I emphasized isothermal values and X = E/RT.)

The constant heating rate relation was

$$-dw/dT = (B/\dot{T})\, e^{-X} \tag{6}$$

and the limits of integration were taken as

$$-\int_1^w dw = (B/\dot{T}) \int_0^T e^{-X}\, dT \tag{7}$$

The constant heating solution of Equation 7 was

$$w = 1 - (BE/R\dot{T})\, p(X) \tag{8}$$

where the function $p(X)$ is defined as

$$p(X) = X^{-1} e^{-X} - \int_X^\infty X^{-1} e^{-X}\, dX \tag{9}$$

and illustrated in Figure 15 (from Reference 15).

A reciprocal relation for the constant rate and isothermal solutions was useful in understanding interrelations

$$X = r(t/t_1)((1 - w_1)/(1 - w))\, e^{+(X_1 - X)} \tag{10}$$

where the constant heating rate $\dot{T}$ appeared implicitly as T and t (Reference 12). For example, a prediction was possible for the weight fraction for a constant-rate experiment, knowing the isothermal

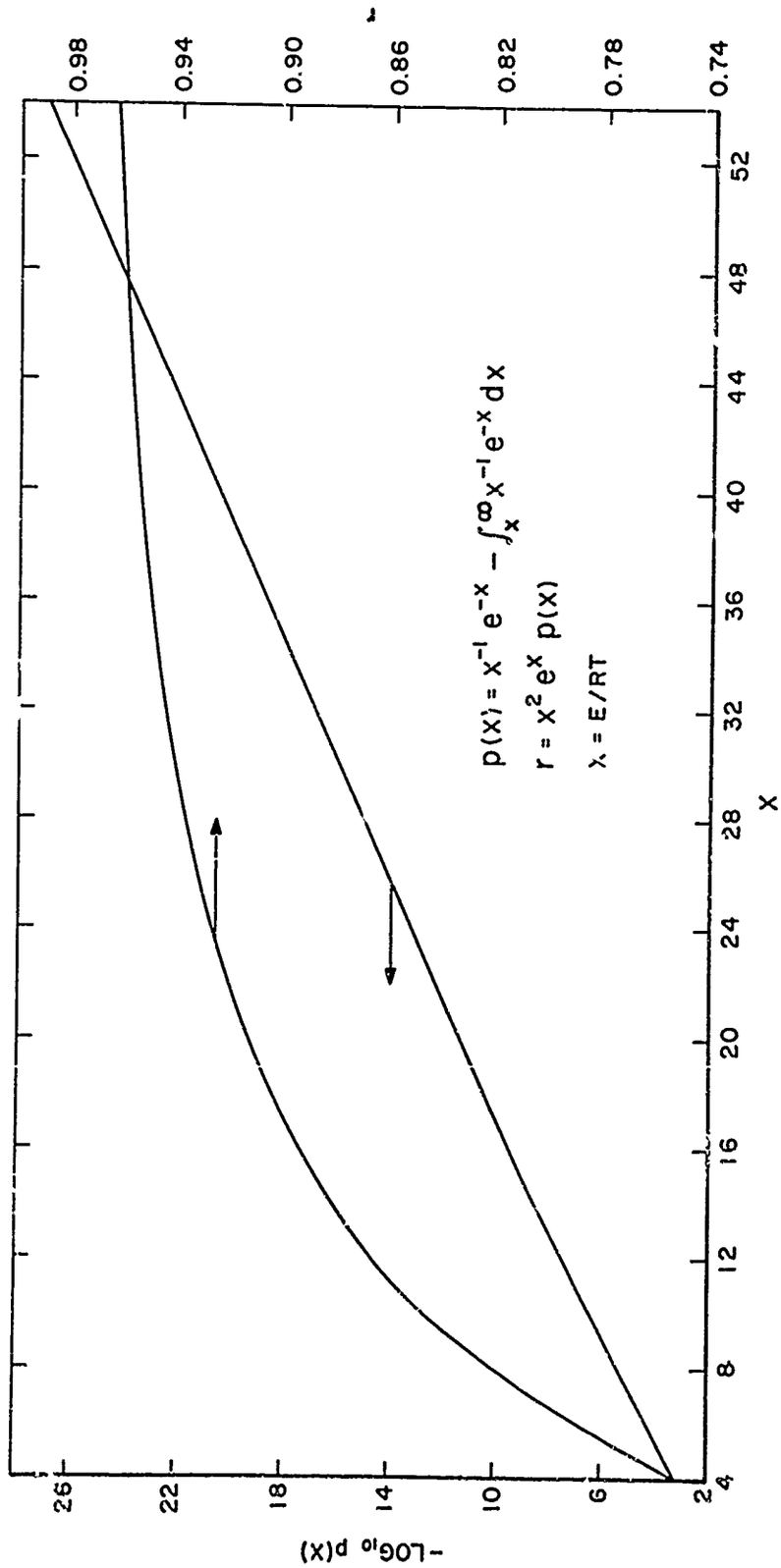

Figure 15. Relationship Between the Terms X, p(X), and r

value for the same period of heating at that temperature via the relations

$$(1 - w) = r(1 - w_1)/X \tag{11}$$

$$r = X^2 e^X p(X) \tag{12}$$

Figure 15 illustrates the relationship between r and X (Reference 15).

The Arrhenius correlation was for constant values of the variables within the lumped term B. In addition to possible changes in other variable values, the surface area of the experimental sample powders was continuously changing during the run. Exact isothermal and constant-heating-rate kinetic solutions were also obtained in closed form for the complete oxidation of poreless graphite spheres. The relations, however, were inconveniently complex for either parametric calculations or other immediately practical use.

No attempt was made to derive a kinetic model for a filled pyrolyzed plastic or graphite. It was clear, however, that it would be difficult to handle pore structure and proportional surface areas. This problem was concluded to perhaps be best amenable to a law of mixtures or other empirical approach.

The Arrhenius correlation was consistent with the phase boundary control mechanism of Reference 1 subject to the proper values of n, A, and E for low temperature surface oxidation. Reference 1 further reviews a variety of models for regions in which transition exists and diffusion dominates.

3. KINETIC CONSTANTS, SAMPLE VARIABLES, AND ENVIRONMENTAL VARIABLES

The kinetic constants n, A, and E ideally reflect the intrinsic oxidative susceptibility of the material. A previous survey gave averaged values for a variety of carbons and graphites. The results were n = 1/2, $A = 1.31 \times 10^6$ gm/atm$^{1/2}$-cm^2-min, and E = 44 Kcal/mole for a terminal surface reactivity control temperature of about 840°C (Reference 2). This value of E was comparable to more recent results for fast kinetics for pyrolytic graphite (Reference 16), a wide variety of carbons, graphites, and pyrolytic graphite (References 6, 17, and 18), and experimental and theoretical results for the low temperature stage of phase boundary control (Reference 1).

The Arrhenius correlation revealed important dependencies upon area, initial weight, oxygen concentration, and pressure. Heating rate was an additional variable for the constant-rate case. The rigorous verification of the basic Arrhenius correlation, the evaluation of A and E, and the evaluation of the n term, all within the lumped B parameter was not easy. It was well known that accurate measurement of weight and temperature along with the precise control of oxygen concentration, pressure, and surface area within minimal experimental error was a difficult undertaking even for the surface reaction control case. There was even greater experimental difficulty for the region of transition and diffusion control.

4. CONSTANT-HEATING-RATE KINETICS PARAMETRIC STUDY

A brief analysis was made for the postulated and unproven kinetics for the constant-heating-rate case. The term $(BE/R\dot{T})$ was parametrically varied over values consistent with possible experiments and materials.

A representative value of $(BE/R\dot{T})$ was 10^{11}. The basis was:

$A = 1.3 \times 10^{6}$ gm/atm$^{\frac{1}{2}}$-cm^{2}-min, $E = 44$ KCal/mole, $P = 1$ atm, $S = 72.5$ cm^{2},

$\dot{T} = 9°C/min$, $w_o = 0.1$ gm, and $z = 0.21$. S was for 0.1 gm of 44-micron-diameter spheres of an 0.94 gm/cm^2 density material.

Thermograms were calculated for $(BE/R\dot{T})$ values of 10^{11}, 10^{12}, and 10^{13} (Figure 16). These values for Equation 8 roughly compensated for the known low estimate for S, uncertainties in A and E, and possible variations in B for other experiments.

The parametric thermograms were displaced toward a higher level of relative thermal stability with decreasing values of the term $(BE/R\dot{T})$. The general shape of each thermogram, however, was relatively independent of the magnitude of this term. There was no maximum rate of weight loss. This was consistent with the original Arrhenius correlation.

5. ANALYTICAL EVALUATION OF ARRHENIUS CONSTANTS

The analysis of isothermal thermogravimetric results to obtain the two Arrhenius constants was a well known procedure. A classical method was to prepare a parametric plot of the linear equation

$$\log_{10}(-dw/dt) = -(E/R \ln 10)(1/T) + \log_{10}B \qquad (13)$$

where the terms $-(E/R \ln 10)$ and $\log_{10}B$ were evaluated as a slope and an intercept, respectively. B and E were then calculated from these two terms.

A wide variety of methods was available for the treatment of constant heating-rate data, including Equation 15 (Reference 19). Of the available computer methods, an approach using matched weight and temperature values to avoid weight-loss rate measurement errors for a nearly linear thermogram was attractive. A computer code widely applied (Reference 19 and 20) for ablative plastic materials was of particular interest for oxidative thermogravimetry and is briefly summarized in the appendix of this report.

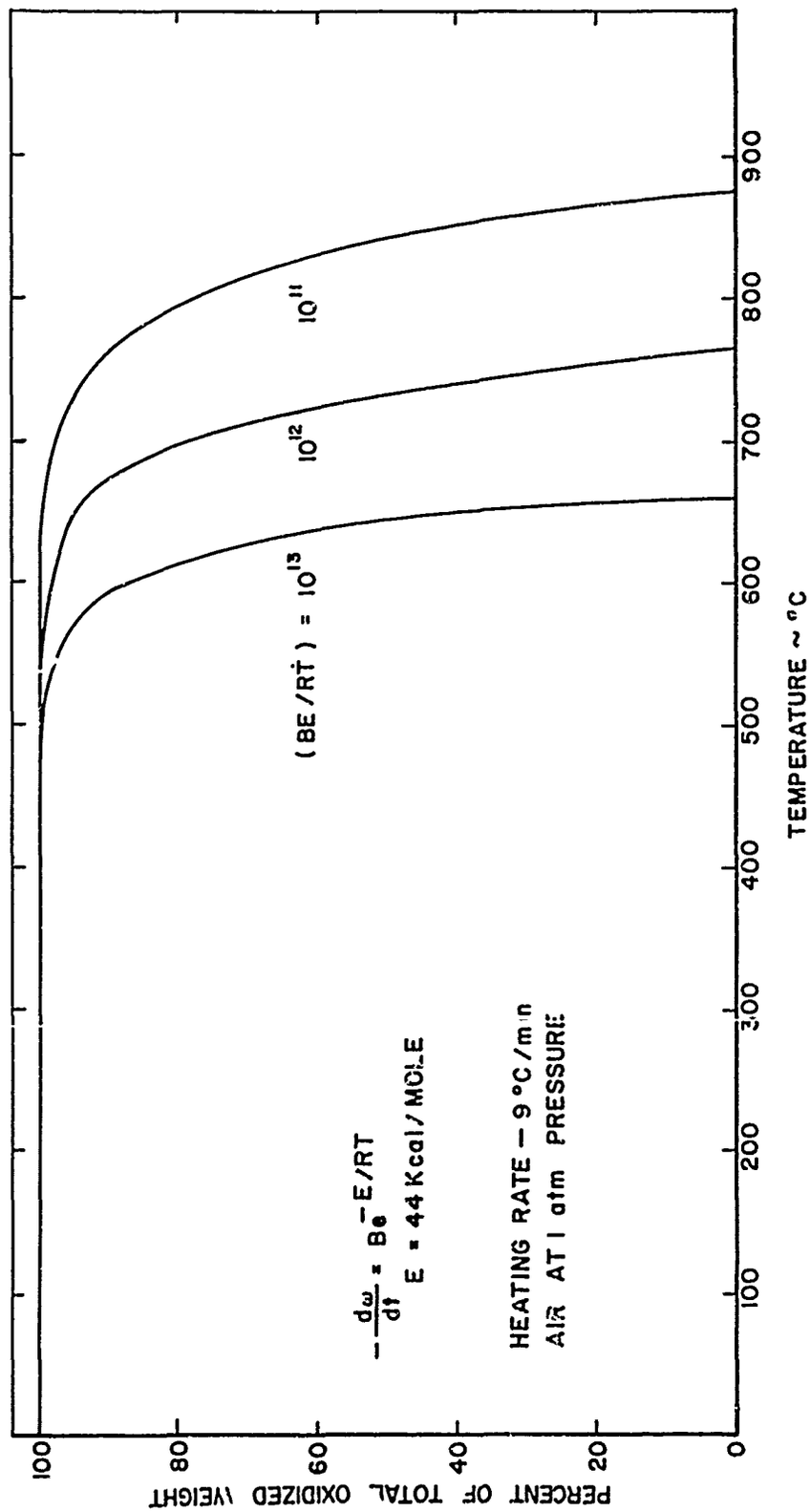

Figure 16. Graphite Oxidation Parametric Study

SECTION VII

SAMPLE AND ENVIRONMENTAL VARIABLES

1. INTRODUCTION

There are a variety of important sample and environmental variables in graphite oxidation. Section VI summarized some general trends for surface reaction, transition, diffusion, and phase boundary control cases.

The complex interplay between variables was more specifically illustrated in two recent studies. In one investigation, isothermal thermogravimetry was conducted for pyrolytic graphite using an Amino Thermo-Grav (References 21 and 22). Samples with one of three surface areas (0.394, 0.927, and 6.27 cm^2) were run at five temperatures, 760, 816, 871, 927, and 982°C, and four airflow rates, 25, 50, 70, and 100 cm/sec (Figure 17). Oxidation rate increased rapidly with temperature for the surface reaction region and was less dependent upon temperature for the diffusion region. In a related but opposite fashion, an increase in airflow rate gave little effect on oxidation rate for the surface reaction case and increased the rate for the diffusion case. The rate further increased with decreasing surface area in both. An unusual result was an increase in transition temperature range with decreasing surface area. This range was between 816-871, 871-927, and above 982°C for the three surface areas. There was little apparent effect of airflow rate on transition temperature range. The Arrhenius constant E was sensitive to the range closely following "breaks" in classical parametric plots of oxidation rate versus 1/T. Unfortunately, the experimental results were not examined in light

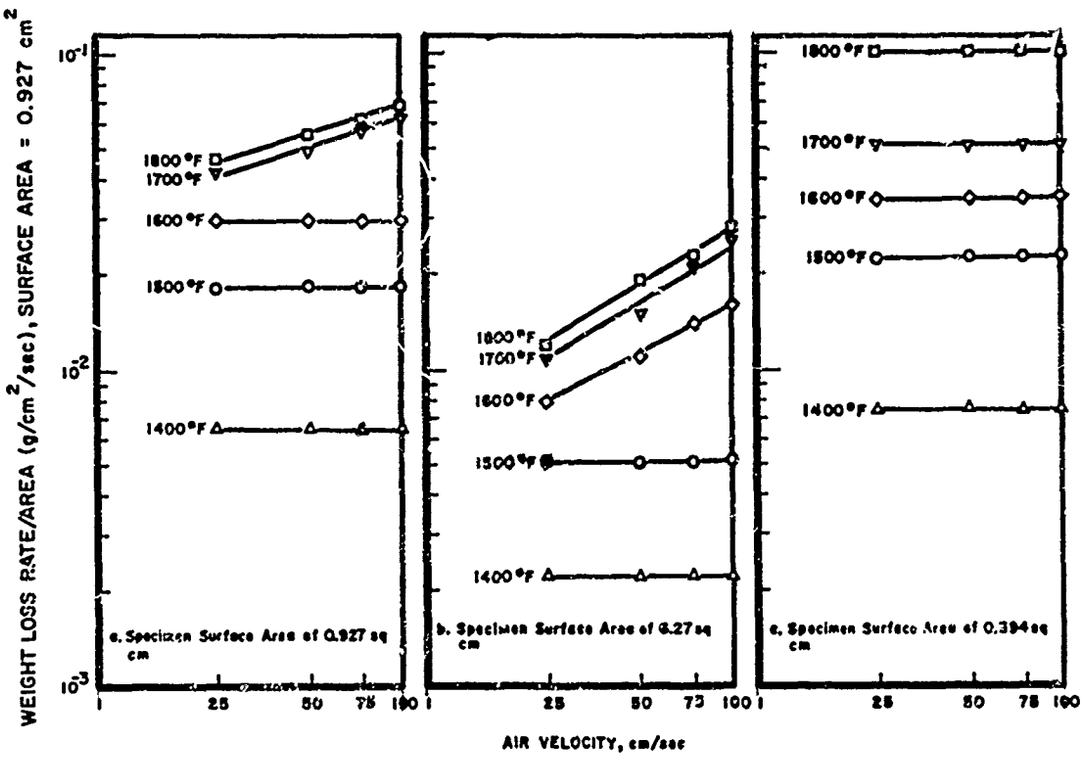

Figure 17. Air Velocity Effects on the Oxidation of Pyrolytic Graphite

of overall phase boundary control mechanism, particularly in terms of (a) oxidation rate dependence upon power of the flow rate (or pressure) and (b) surface area effects.

A variety of methods was applied in an investigation at the higher temperatures where diffusion was a major effect (Reference 1). The techniques included low velocity tests in resistance heated tube furnaces, low velocity tests of inductively heated samples, high velocity tests of inductively heated samples, and air arc heater tests extending into sublimation control. The materials included a glassy carbon, five graphites, and a pyrolyzed plastic. There were few low temperature measurements. Oxidation rates were insensitive to temperature above about 1540°C and dependent upon flow at rates higher than an onset value of about 220 cm/sec. Extensive studies were made at the higher temperatures to evaluate the effects of gas velocity, material type, sample configuration, and temperature. Similar oxidation rates were found for three different graphites; there was minor apparent effect of minor variations in density, porosity, purity, and structure on oxidative rate. Rate differences were found, however, for the significantly lower densities of the glassy carbon and pyrolyzed plastic. Thirty-degree conical samples were necessary to avoid the shape changes found for flat face and hemispherical configurations. Preliminary supporting evidence was presented for a phase boundary control mechanism primarly in such terms as differential oxidative rates for the dominant planes of anisotropy of pyrolytic graphite, E dependence upon temperature, existing kinetic models, and oxidation rate dependence upon flow rate (or surface oxygen partial pressure).

References 1, 21, and 22 represent two examples of recent work particularly relevant to the postulated features of phase boundary control. There were a large number of additional previous studies well illustrating the critical aspects of sample and environmental variables. A review of this literature was far beyond the scope of this report. Other important studies and reviews, for example, include References 2, 16, 23, 24, 25, and 26.

This section details important sample and environmental variables uncovered in this preliminary study. There was emphasis in understanding fundamental interrelationships in terms of the Arrhenius kinetic correlation and in planning approaches to more detailed understanding in any future work.

2. SAMPLE CONFIGURATION

Fine powders were used primarily to maximize oxidation rate in a "worst case" sense in this preliminary work. First, the kinetic analysis revealed higher oxidation rate for the higher surface area of a fine powder. Secondly, the diffusion of gaseous phases was probably promoted by fine powders. Intradiffusion amidst particles and perhaps interdiffusion within particle pores should have further increased oxidation rate. Any equilization of surface and pore structure by grinding should have suppressed intrinsic oxidation resistance between the different materials.

There was an additional practical problem in using a solid sample configuration. The limited quantity of available materials, their small sizes, and attendant machining aspects were additional restrictions.

The experimental results revealed that fine powders promoted oxidation. For example, the ammonium chloride filled pyrolyzed plastic was run in three particle sizes (Figure 18). These included: a bulk particle, as-ground powder, and sieved powder. More oxidation was found with decreasing particle size.

The most significant effect of particle size was for a swatch of WCB graphite fabric compared to -325 sieve powder prepared by grinding the fabric (Figure 18). The result was consistent with expected faster oxidation for an increased total surface area.

The surface area variability between materials was probably suppressed by grinding. The sieved particles were less than a limiting dimension of 44 microns in size. The particle distribution scale was unknown.

A typical poreless surface area was 72.5 cm^2 for a 100 mg sample of perfect spheres. A typical measured surface area was $2x10^5$ cm^2 for the same weight of pyrolyzed plastic powder. There was little doubt that only a small fraction of the available area was subject to oxidation during thermogravimetry. To a limited degree, the similarity of many oxidation thermograms was consistent with the similarity of internal pore structure of bulk particles within two material classes of "wide" and "narrow" distributions of relative pore volume (Section VIII).

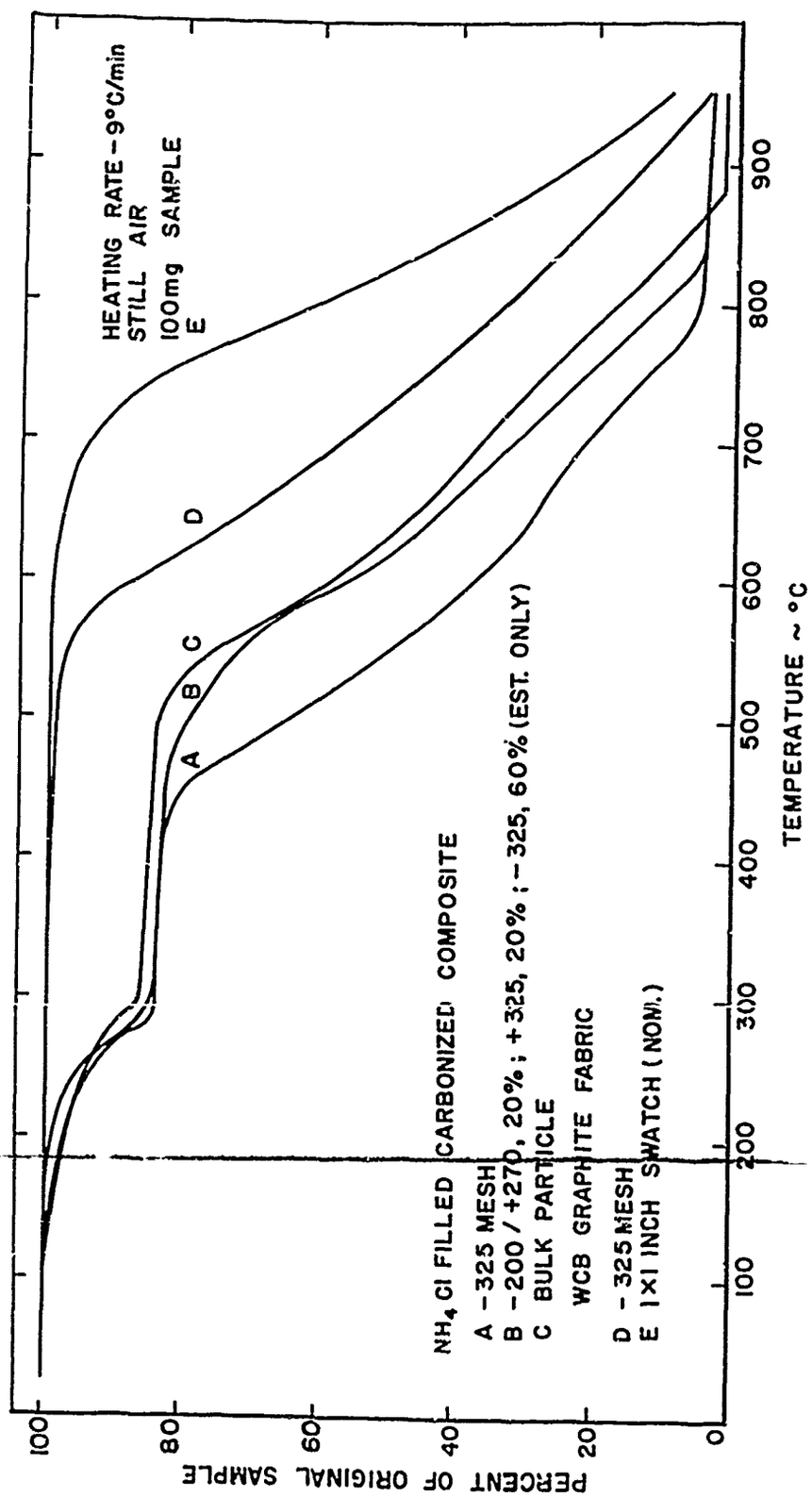

Figure 18. Particle Size Effects for Various Materials

The apparent minor effect of surface area of powders (but not particle size of particles) was somewhat consistent with some previous results. Reference 14 reported a relative minor effect for the thermogravimetry of two otherwise similar carbon cloths with widely varying surface areas (Figure 19). Isothermal thermogravimetry likewise gave little obvious surface area effect.

A sample with a constant surface area and equilibrium internal pore structure was desirable for practical kinetic analysis. While extremely difficult to achieve experimentally and maintain for a long time, a receding flat face approached an ideal surface area (Reference 1). The existence of an equilibrium pore structure obviously required detailed study for specific materials.

The similarity of response of many materials was not a direct result of oxygen "starvation" of the sample limiting oxidation or causing other defective aspects of the experiment. This was well illustrated by other routine constant-heating rate and isothermal runs on a wide variety of samples. Figures 20 and 21 illustrate the diversity of oxidation behavior of carbonaceous and graphitic fabrics resulting from varying degrees of carbonization of the precursor material. Figure 22 shows the effects of a yarn, bar, or whisker form of carbon or graphite of unspecified nature. Figure 23 illustrates the protective effect of oxidation resistant coatings applied to a carbon fabric.

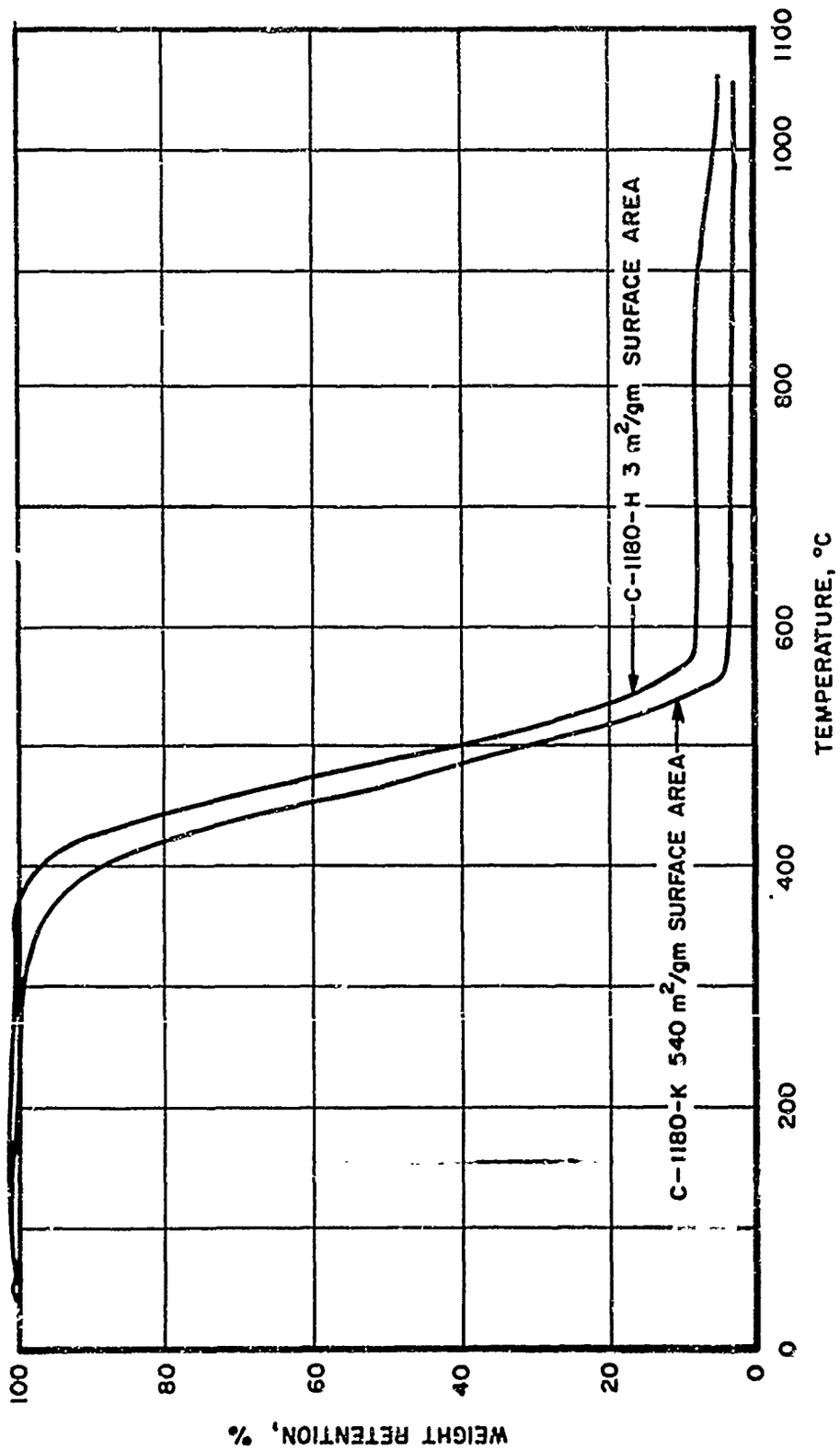

Figure 19. Surface Area Effects for Two Carbon Fabrics

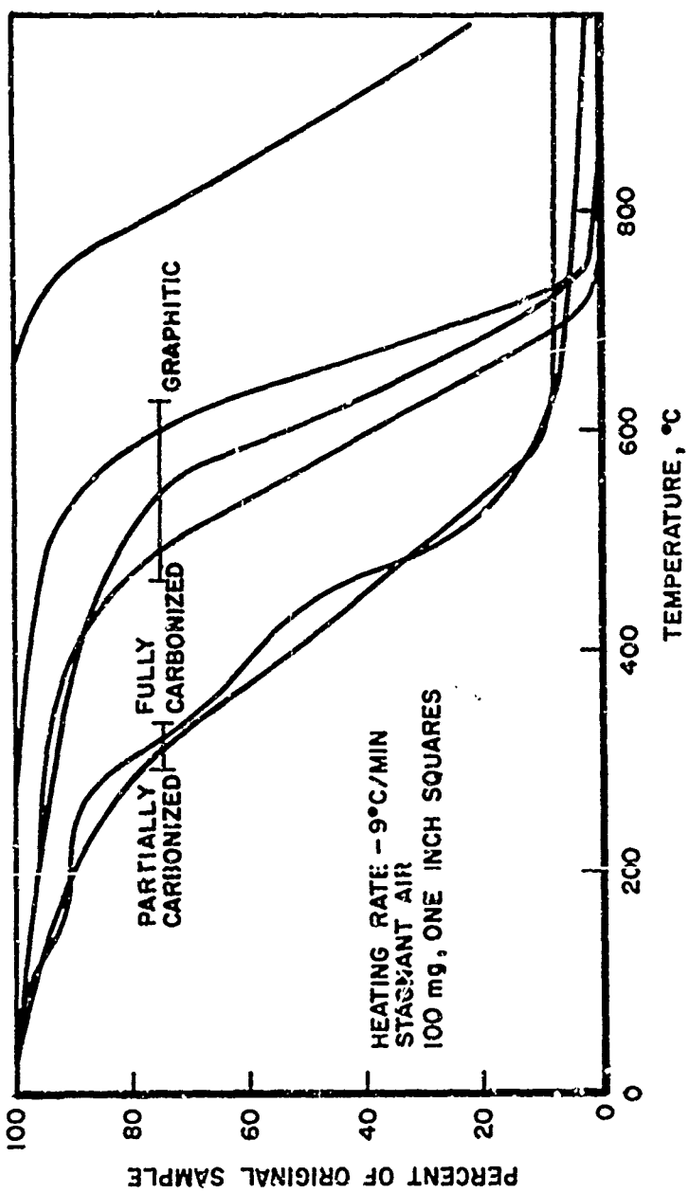

Figure 20. Constant Heating Rate Thermograms for Carbonaceous and Graphitic Fabrics

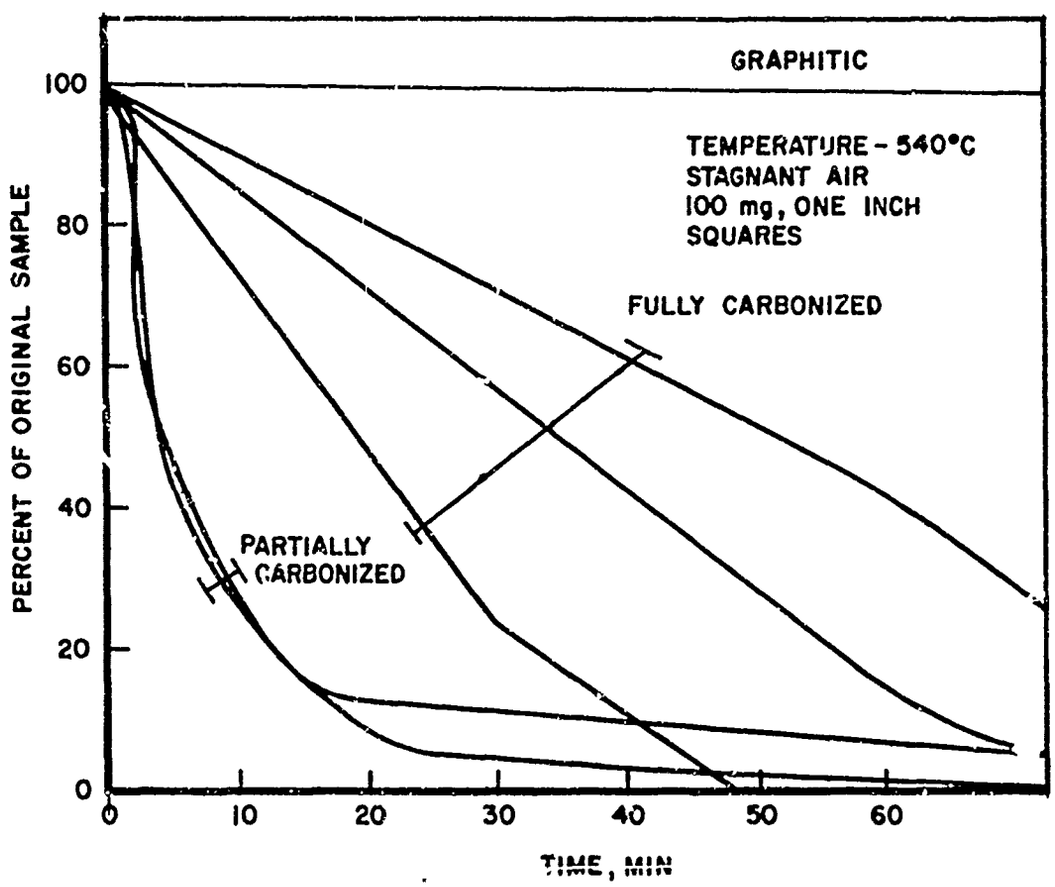

Figure 21. Isothermal Thermograms for Carbonaceous and Graphitic Fabrics

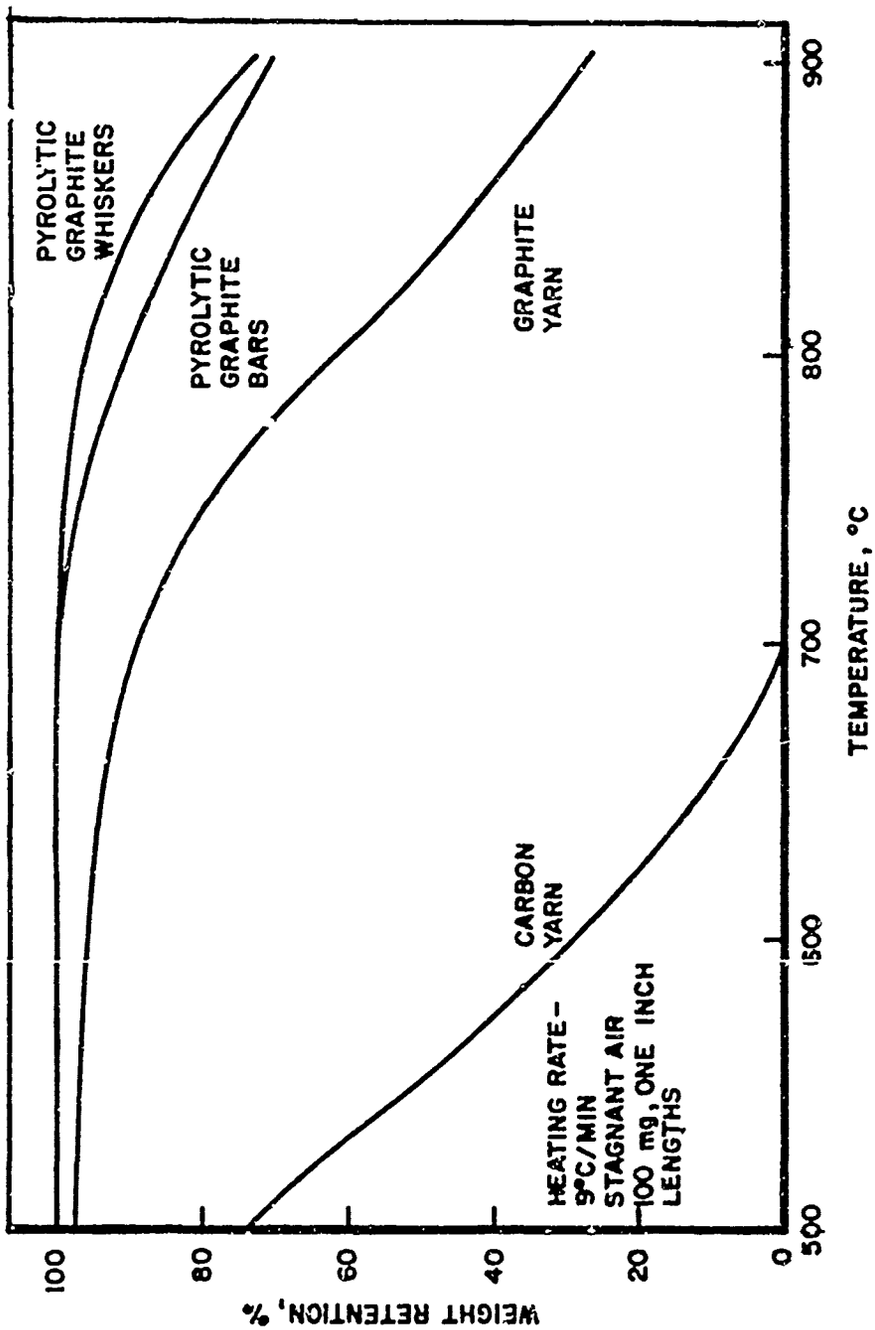

Figure 22. Thermograms for Carbonaceous and Graphitic Materials

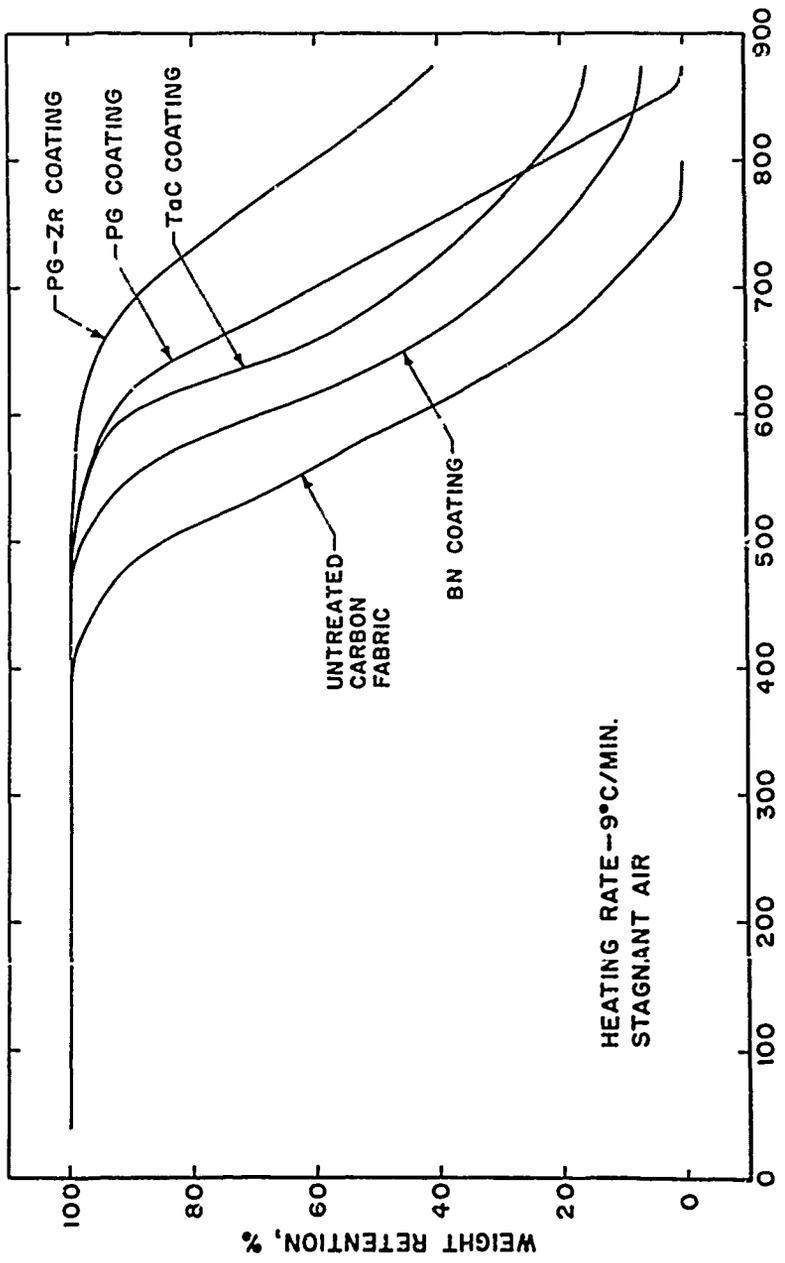

Figure 23. Thermograms for Coated Carbon Fabrics

3. OXYGEN CONCENTRATION AND PRESSURE

Systematic variations were one approach to studying oxygen concentration and pressure, either to clarify mechanisms, for kinetic analysis, or empirical' . The use of different gases of varying oxygen content was a means of varying concentration. The chamber pressure was adjustable over certain ranges. It proved difficult, however, to maintain both oxygen concentration and pressure at constant levels during the run.

The quantity of air necessary for oxidation of a 100 mg sample of carbon was approximately equal to 0.6 of the volume of the weighing column. For the standard run, therefore, local sample consumption probably exceeded the supply by convection currents. Runs in other gases were subject to the same problem although to a lesser degree if the initial oxygen concentration was higher than for air. A reduced pressure run began with essentially the same oxygen concentration as for air but with considerably less available oxygen. A practical method for studying both oxygen concentration effects in spite of these handicaps was by gas-purging runs at atmospheric and reduced pressure.

AGKSP graphite powders were run in an air purge and in initially quiescent air (Figure 24). Lower thermal stability was found for the 1 liter/ min air-purge run. This implied a changing oxygen concentration for the standard run above 750°C where the two thermograms began to converge.

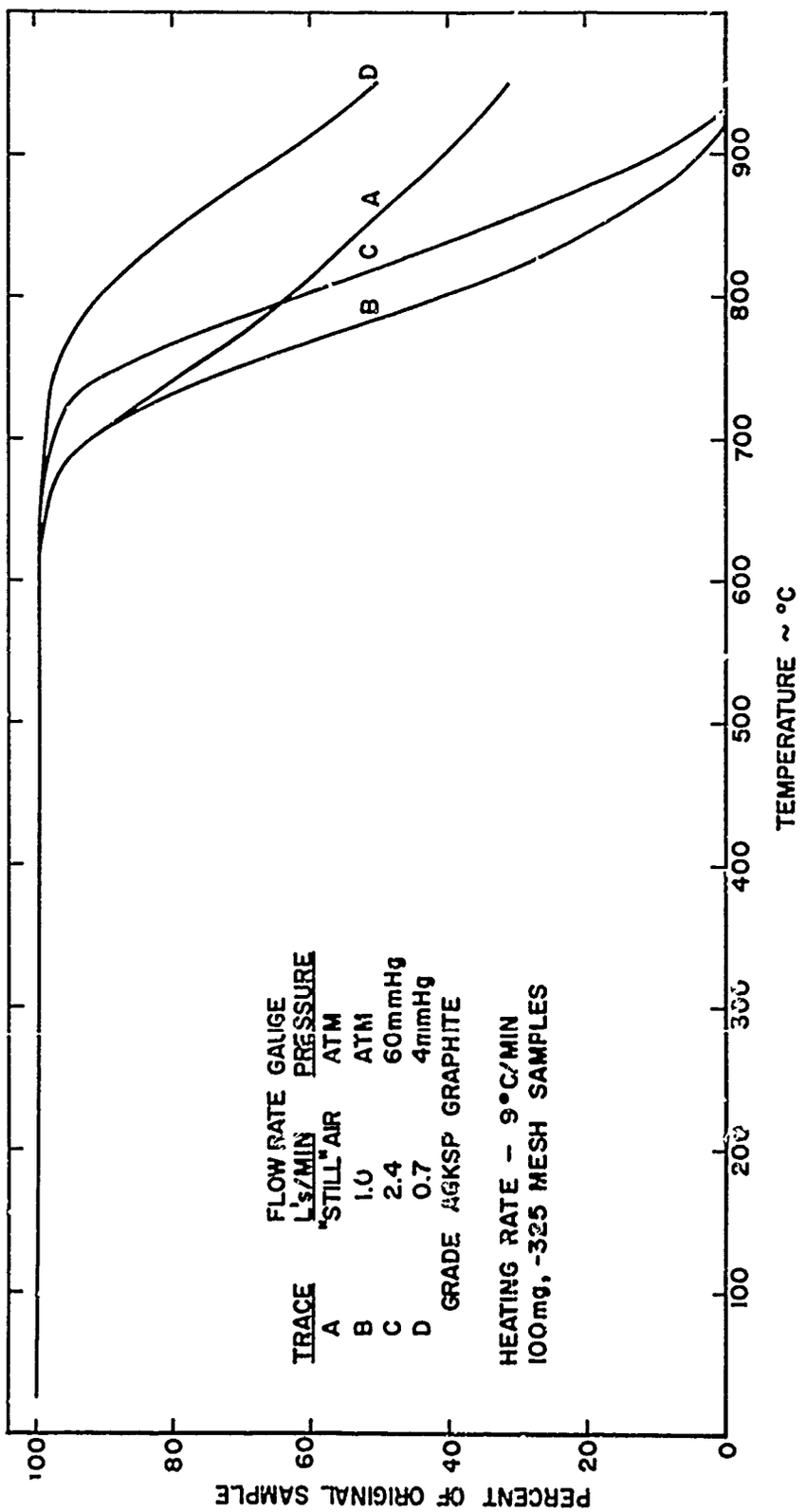

Figure 24. Airflow Rate and Pressure Effects for a Graphite

AGKSP air-purging runs at reduced pressure were consistent with expected increased oxidation at a higher flow rate (Figure 24). The results were also consistent with reduced oxidation with a decrease in pressure.

A sufficiently high airflow rate, at either ambient or reduced pressure, promised a reduction of changes in oxygen concentration. The limiting levels of either flow rate or pressure for the AGKSP runs, however, were at the extremes of stable operation of the thermobalance.

A prototype gas-purge/vacuum network was assembled to give controlled levels of flow rate and pressure over wide ranges with stable operation (Figure 25). The control and stability performance of this version of the apparatus of Reference 23 was reasonably good in checkout runs.

For the prototype apparatus, the inlet flow rate into the crucible chamber was regulated by glass capillary tubes. The inlet gas was preheated by passage down a tube on the chamber wall before free injection just below the crucible.

Pressure was controlled by a sensitive Cartesian diver manostat. An insensitive vacuum regulator permitted gross adjustments. In addition, the regulator pressurized the capillary tubes for better regulation and permitted direct reading of the rotameter. A differential manometer was used for visual monitoring of pressure fluctuation during the run. Injection of a second gas at the manostat was an optional means of controlling any large fluctuation.

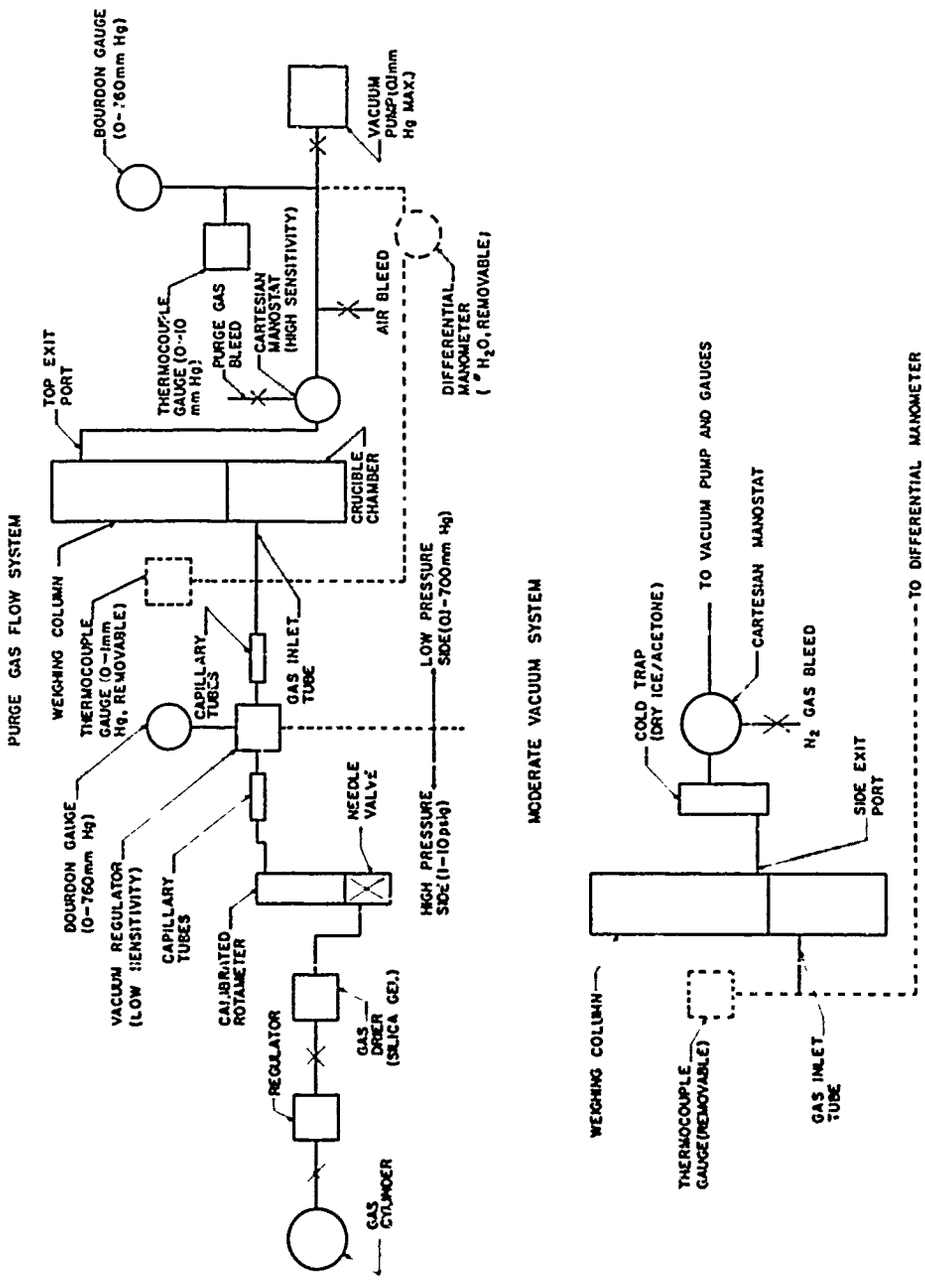

Figure 25. Prototype Flow Rate and Pressure Control Network

4. HEATING RATE

The pyrolyzed plastic was run at heating rates of 3°C/min and 9°C/min (Figure 26). There was little similarity between the two thermograms. The reference temperature for 50% weight loss dropped from about 660°C at the higher rate to near 570°C at the lower one.

A change in surface oxygen concentration was a possible factor in the unexpectedly large heating rate dependence. The long "tail" for the 9°C/min run and the absence of this region at 3°C/min was consistent with possible changing oxygen concentration at the higher rate.

Additional runs were desirable for probing heating rate and any attendant effects as for oxygen concentration change. Unfortunately, the 3°C/min rate was the lowest available. The highest useful rate of 9°C/min was convenient for looking at a large number of materials.

5. OVERALL OXIDATION MECHANISMS

There was considerable evidence of important diffusion effects and perhaps a dominant phase boundary control mechanism for constant-heating-rate thermogravimetry. First, the temperature rate of weight loss was nearly constant following a low temperature period. Secondly, there was little difference between the materials excluding AGKSP. These two results were strongly characteristic of diffusion effects.

In addition to two results consistent with apparent diffusion effects, there were several additional observations concerning overall mechanisms. The constant-heating-rate experiment was, first of all, significantly

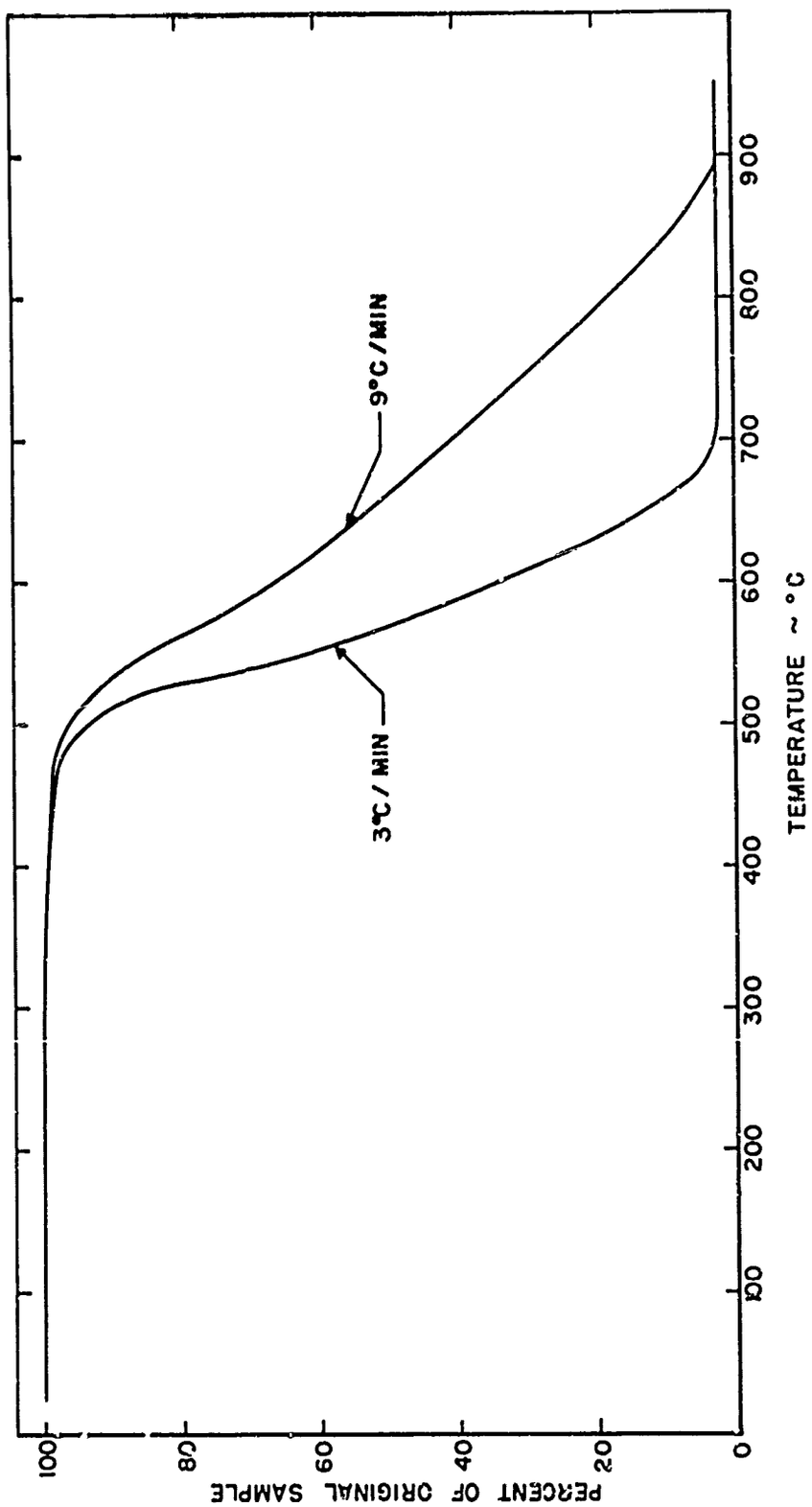

Figure 26. Heating Rate Effects for a Pyrolyzed Plastic

different from the conventional isothermal run for a solid sample. The steadily decreasing quantity of sample powder consumed a steadily decreasing total quantity of oxygen. Although oxygen shortage may have prevented a transitional "tripping" as it did for the conventional isothermal case, there was also a tendency toward oxygen concentration equilibrium if diffusion effects were already important. There was little doubt that the large sample powder surface area promoted early diffusion effects in a low temperature transitional range (Reference 21). The fact that oxidation rates were found to be higher at the higher air flow rates and lower at the lower pressures for AGKSP primary runs was further evidence of diffusion effects (Figure 24). The higher oxidation rates were more characteristic of diffusion than of surface reaction (Figure 24). The distinct differences for runs at two heating rates suggested important diffusion effects at the higher rate and surface reaction effects at the lower (Figure 26).

The overall conclusion for sample and environmental variables was a capability of giving the external appearances of true diffusion control without necessarily having true control. There were two factors that were not consistent with true control. The first was an apparently paradoxical result of surface reaction effects occurring at higher temperatures than did the diffusion effects for four runs for AGKSP (Figure 24). The second was a steady decrease in the surface transfer of the limited quantity of oxygen in the thermobalance at the higher run temperatures. This loss of oxygen could have lead to oxygen "starvation" of the sample at a near constant surface concentration. Starvation was similar in some respects to the "supply limited" cases of Reference 1 (Figure 9).

The apparent ability to provide external appearances of shifting surface reaction versus diffusion effects by shifting sample and environmental variables was consistent with the overall phase boundary control mechanism of Reference 1. The sample and environmental variables of material type (n, A, E), airflow rate (n, z, P), oxygen concentration (n, z, P), heating rate (t, T, $\dot{T}$), pressure (P), surface area (S), and initial weight (w_o) corresponded to terms in the Arrhenius kinetic format. Therefore, there was little reason not to expect transition to be apparently kinetically dependent to varying degrees. Several cases were postulated as examples. Theoretically, the "onset" temperature was only dependent upon time for the condition of transition occurring at the same rate of oxidation, or oxygen consumption, for both isothermal and constant-heating-rate cases for a fixed value of the parameter B. Another criterion was for transition to occur only after a fixed, "onset" quantity of oxygen was consumed from a starved system. Then taking transition to be dependent upon oxidized weight and an isothermal temperature of 800°C, the reciprocal relation (Equation 10) gave 980°C for E = 44 Kcal/mole and $\dot{T}$ = 9°C/min. Or stated another way, a constant heating rate slowed oxidation to the point that 980°C was necessary to lose the same material lost at 800°C for the same total time. As a final case of three, transition was postulated to be completely dependent upon kinetics. Transition was then dependent upon B, temperature, time, and weight for the isothermal case and further dependent upon the term ($BE/R\dot{T}$) for the constant-heating-rate case (Equations 5 and 8).

The value of E is temperature dependent for phase boundary control (Reference 1). The transition temperature was reduced to a single value for true kinetic dependence by considering a step-change in E. The effective result was w = 0. For the constant-heating-rate case, typical results were about 600, 770, and 880°C for $(BE/R\dot{T}) = 10^{13}$, 10^{12}, and 10^{11}, respectively (Equation 8). Isothermal onset temperatures were readily available from Equation 5 for this step-change.

There were several runs where the rate of sample oxidation went through a minimum value. The materials were a pyrolyzed plastic particle, graphite fabric, graphite fabric powder, and AGKSP graphite powder (Figures 12 and 13). The minimum rate was unexpected in that this implied a possible change in rate-controlling mechanism. The minor deviation possible, experimental error, and irregular oxidation were possible factors in this result.

A versatile thermobalance capable of systematic variations in airflow rate, heating rate, oxygen concentration, pressure, surface area, and weight was a potential means of analysis of phase boundary control or other oxidation mechanisms for either isothermal or constant-heating-rate thermogravimetry. This preliminary work suggested that limited shifts in a few sample and environmental variables resulted in apparently corresponding but still to be fully explained shifts in surface reaction effects and diffusion effects.

SECTION VIII

PHYSICAL PROPERTIES

1. DENSITY, POROSITY, AND PORE SPECTRA

Density and porosity were examined using a mercury intrusion porosimeter. This instrument was manufactured by the American Instrument Company. The operational procedure and physical arrangement were described in detail in Reference 27.

The similarity of the oxidation thermograms of the pyrolyzed plastics, carbons, and graphites was remarkable in view of the wide ranges of densities and porosities (Table II). The nominal limiting values were 0.5-1.0 gm/cc for apparent density, 1.5-2.0 gm/cc for true density, and 24-70% for total porosity.

The materials were roughly classed as having "wide" and "narrow" distributions of pore volume as a function of mean pore diameter (Figure 27). In contrast to the highly irregular cells of the pyrolyzed plastics, the commercial carbons and graphites had nearly equal concentrations of a wide range of cell sizes. This was attributed to a known open, interlocked cell structure (Reference 28).

The thermogravimetry samples were prepared by cryogenic pulverization. The particle major dimension was 44 microns. The density, porosity, and pore spectra characteristics of the samples were therefore somewhat different from the bulk particles used for porosimetric measurements.

TABLE II

PHYSICAL PROPERTIES

Material/Property	Apparent Density (gm/cc)	True Density (gm/cc)	Total Porosity (percent)	Apparent Specific* Surface Area (m^2/gm)
Pyrolyzed Plastic	0.94	1.50	37.2	220
Pyrolyzed Plastic (-325 sieve powder)				200
Pyrolyzed Plastic, Ammonium Chloride	1.13	1.54	23.9	
WCB Graphite Fabric	0.48	1.58	69.7	3**
Grade 20 Porous Carbon	1.10	2.01	45.4	
Grade 40 Porous Carbon	1.00	2.00	49.8	0.5
Grade 20 Porous Graphite	1.10	2.04	46.0	

*BET method and pretreatment of 3 hours at 350°C in dry helium unless noted.

**Manufacturers data.

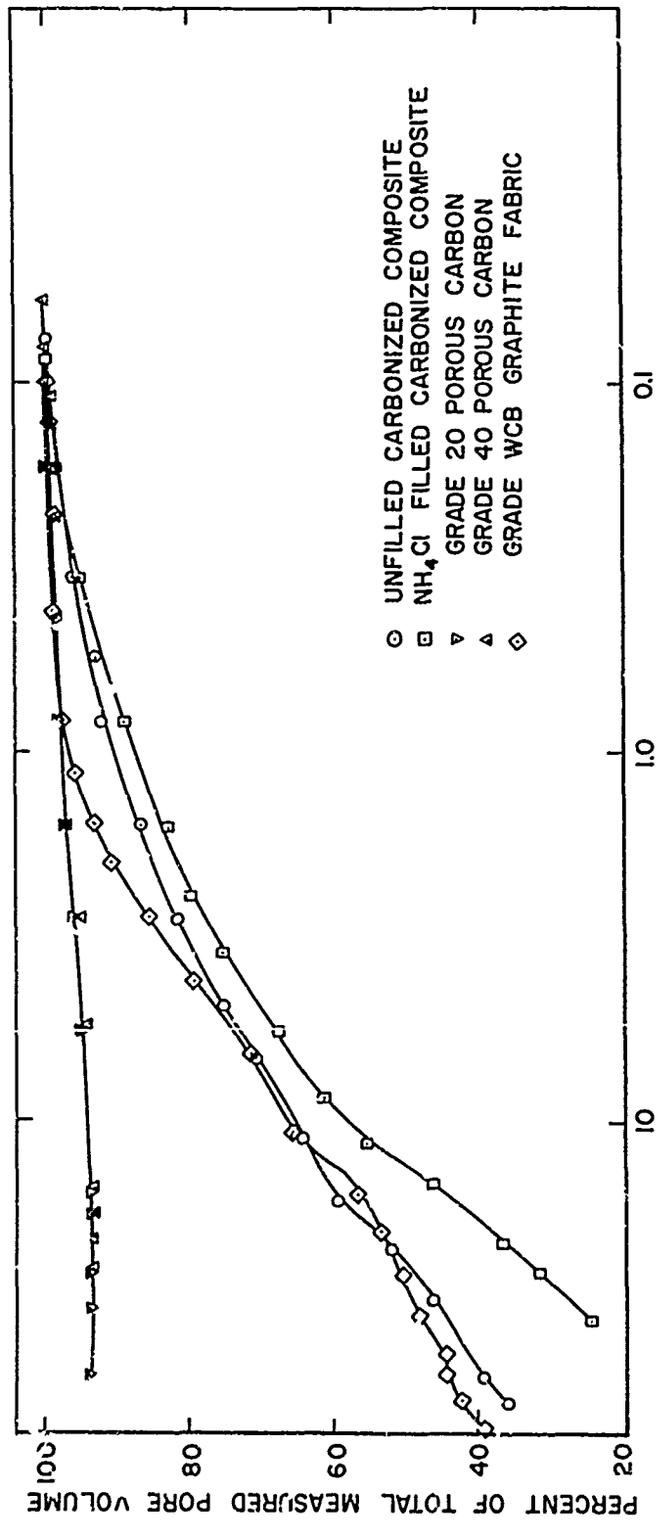

Figure 27. Pore Spectra for Various Materials

The pore spectra for Grade 40 porous graphite was nearly identical to the results for the two porous carbon grades (Figure 27). The density and total porosity results for all porous carbons and graphites agreed well with handbook values (Reference 27). The pore spectra for the pyrolyzed plastic was in good agreement with a distribution for a similar material (Reference 12).

2. SPECIFIC SURFACE AREA

Specific surface area was examined using a nitrogen absorption Sorptometer. This instrument was manufactured by the Perkin-Elmer Corporation. General procedures for similar measurements were detailed in Reference 29.

The specific surface areas of the pyrolyzed plastic were relatively high (Table II). The results were 220 m^2/gm as a bulk particle and 200 m^2/gm as a fine powder for a reference pretreatment condition.

There was a strong dependence of absorption measurements upon pretreatment. As an example, "apparent" specific surface areas of 12, 40, 160, and 220 m^2/gm were found for four bulk particles of the pyrolyzed plastic for pretreatment in a helium purge for three hours at room temperature, 80, 100, and 350°C. These values were for either a one-point estimate or a three-point evaluation of a classical Brunauer-Emmett-Teller (BET) parametric plot. The 220 m^2/gm value was held to be the most valid as approaching a true specific surface area.

High temperature pretreatment was not possible for the ammonium chloride filled pyrolyzed plastic due to filler pyrolysis. Estimates were made, however, as a point of interest for three bulk particles after helium pretreatment for three hours at room temperature, at 80, and 100°C. The apparent results were roughly 0.1 of the normal composite for equivalent pretreatments. There was evidence of minor filler decomposition for the 100°C degassing.

The strong dependence of apparent specific surface area upon pretreatment conditions was possibly associated with more efficient removal of absorbed vapors at the higher temperatures, the opening of fissures, surface "activation," or other unknown aspects.

Apparent specific surface area dependence upon temperature implied that an equilibrium internal pore structure may not exist. A further implication was that there were gross uncertainties in Arrhenius constants due to pore structure variations during thermogravimetry. If an equilibrium structure was possible, the pretreatment prior to the experiment was desirable. On the other hand, the similarity of the oxidation thermograms for the different materials implied that variable pore structure was possibly an insignificant factor, masked by other effects, or the equilibrium structure was perhaps approached while heating up.

SECTION IX

ACCURACY, PRECISION, AND SENSITIVITY

1. RLSIDUAL WEIGHT

There was a linear and reproducible weight loss error from 600-950°C for quiescent air runs. The thermograms were not corrected for the small error of up to 3/4% maximum at 950°C. No error was found for air purging runs at reduced pressure. A near linear weight loss error for vacuum runs resulted in a maximum deviation of about 4% at 950°C. All vacuum thermograms were corrected for this error.

The error in air was primarily due to electrical component drift. The error in vacuum was attributed to buoyancy force increase due to pressure increase while heating and electrical component drift. The buoyancy force error was later eliminated with a Cartesian diver manostat that gave a near constant pressure.

A parasitic weight error found during early work with the Thermo-Grav was attributed to overheating of the springs. This error was eliminated by using cooling blowers to maintain temperature equilibrium.

2. REFERENCE TEMPERATURE

Temperature errors were associated with thermal gradients for the crucible, sample, and the reference thermocouple. There were additional thermocouple calibration errors.

The reference thermocouple was located in a quartz sheath about 3/4 inch directly below the crucible. A second thermocouple was bonded into a crucible with ceramic cement. The differential temperature was recorded as a function of reference temperature (RT) for a 9°C/min run in quiescent air. The RT exceeded the crucible temperature (CT) by up to about 7°C (Figure 28).

Differential temperature runs were made with 100 mg samples of the pyrolyzed plastic and filled composite. The CT first approached and then exceeded the RT by up to 8°C during exothermic oxidation of the pyrolyzed plastic. The ammonium chloride filler gave an expected endothermic cooling during pyrolysis.

The two Chromel alumel thermocouples were calibrated against a platinum, platinum + 10% rhodium standard thermocouple (ST). The ST was certified by the National Bureau of Standards. The independent variable was the normally recorded RT and the dependent variables were corrections. The corrected RT_c and CT_c conformed to the relations

$$RT_c = RT - (RT - ST) \tag{14}$$

$$CT_c = RT_c - (RT - CT) \tag{15}$$

The corrected crucible and reference temperature differences ranged as high as ± 10°C for the pyrolyzed plastics. In view of possible additional error due to poor thermocouple contact and a thermal gradient for the crucible and sample, this value was considered conservatively low.

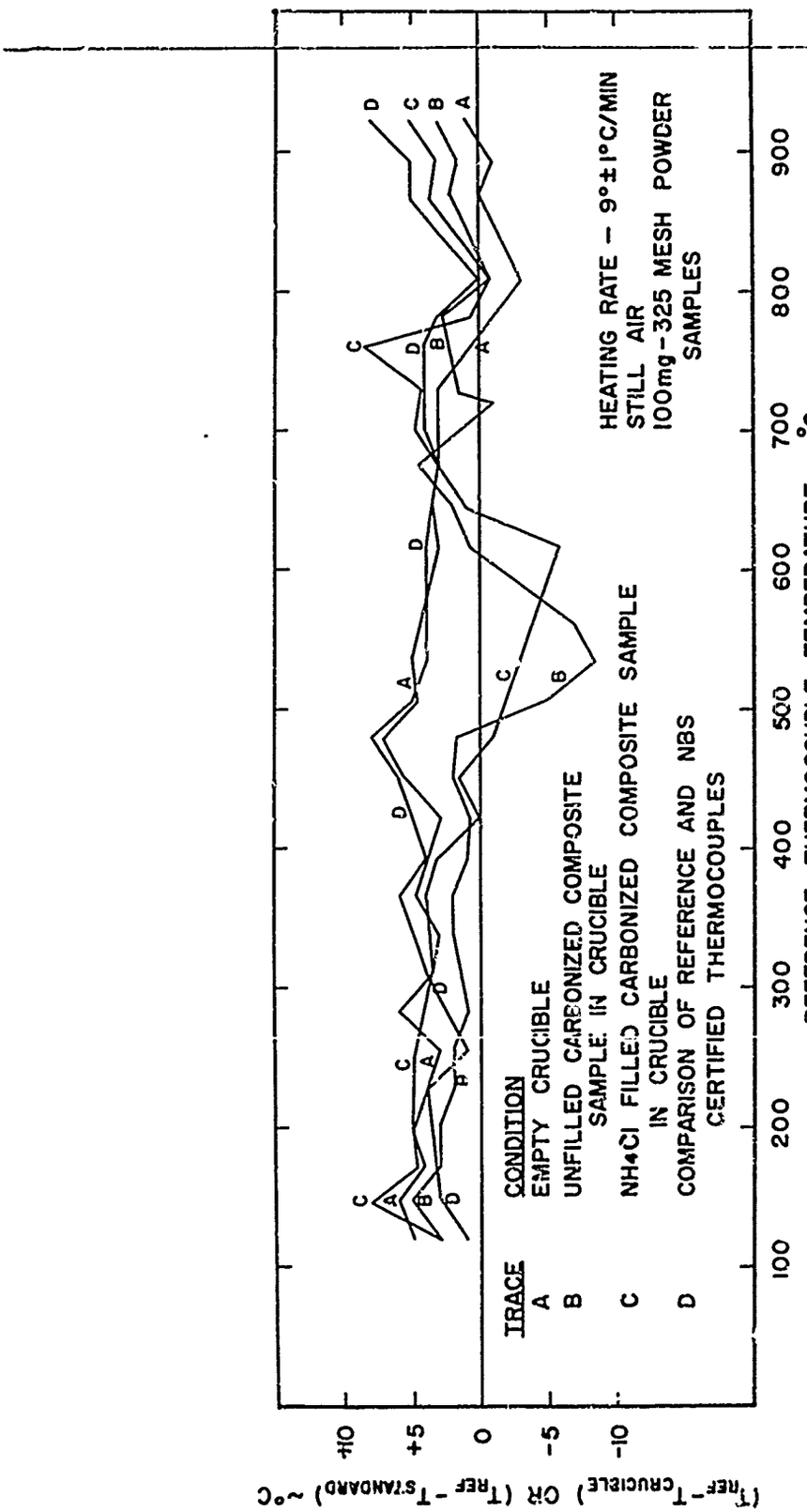

Figure 28. Reference Thermocouple Calibration Curves

3. THERMOGRAM REPRODUCIBILITY

Duplicate oxidation thermograms revealed reproducibility of a sample run within a few weight percent (Figure 29). An average difference of about 6% by weight was found for thermograms for two different samples of the pyrolyzed plastic. The reasons for this large imprecision were unknown but could have been associated with imperfect grinding or sieving operations.

4. PHYSICAL PROPERTIES

A detailed analysis of porosimetric errors led to typical maximum values for carbonaceous materials: $\pm$0.05 gm/cc for apparent density, $\pm$0.10 gm/cc for true density, and $\pm$6% for total porosity (Reference 27). The results for the commercial carbon and graphite porous grades were in excellent agreement with other measurements (Reference 28). The absolute accuracy of porosimetry was limited to some degree by the inaccessibility of pores with mean diameters above about 10 microns.

The nature and magnitude of errors for typical nitrogen absorption measurements were described in detail elsewhere (Reference 29).

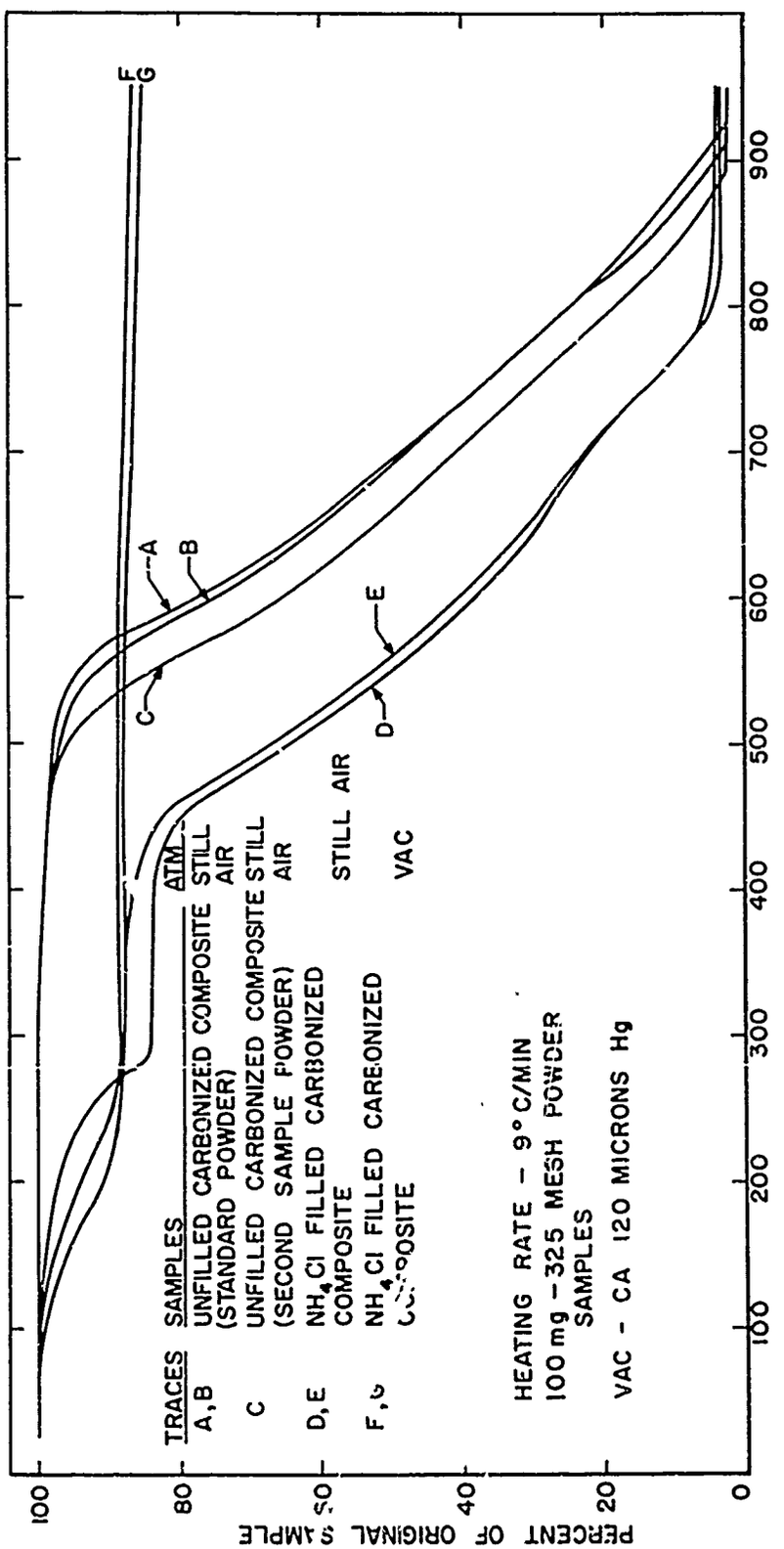

Figure 29. Thermograms for Duplicate Runs

SECTION X

SUMMARY OF THE ACTUAL EXPERIMENTAL WORK

Constant-heating-rate thermogravimetry was conducted in air for two pyrolyzed plastics, three graphites, a graphite fabric, and a carbon material. All sample powders gave similar thermograms except a high density, high purity graphite and a filled pyrolyzed plastic.

A number of procedural variables proved significant. An increase in airflow rate, heating rate, oxygen concentration, pressure, or surface area gave decreased oxidative resistance. The materials fell within either "wide" or "narrow" distributions of pore volume. Both classes gave similar thermograms. The sample and environmental effects were partially consistent with the external appearances of diffusion control of oxidation. These external appearances were tentatively attributed to phase boundary control of graphite oxidation.

The thermobalance was inadequate for detailed study of sample and environmental variables. There were limitations on the operational ranges of airflow rate, heating rate, oxygen concentration, and pressure. A prototype gas-purge/vacuum network was successfully built to extend capabilities. A versatile thermobalance capable of detailed study of sample and environmental variables over wide ranges was considered a potential means of confirmation of phase boundary control of graphite oxidation.

An isothermal relation in an Arrhenius format was solved for a constant-heating-rate run of a constant surface area sample. The indicated trends of decreasing oxidation resistance with increasing oxygen concentration, pressure, or surface area were reasonably consistent with the experimental thermograms. The experiments were not designed for Arrhenius constants evaluation and no attempt was made to do so.

The weights of a pyrolyzed plastic and ammonium chloride were essentially additive, by a law of mixtures, to give the hermograms of an ammonium chloride filled pyrolyzed plastic in both air and vacuum.

Density, porosity, pore spectra, and specific surface area were examined for selected materials. There were wide ranges of densities and porosities. The pore spectra largely fell within two general classes. Specific surface areas were strongly dependent upon the method of sample pretreatment.

The standard thermogravimetry run was for a -325 sieve, dried 100 mg powder at 9°C/min to 950°C in initially quiescent air. There were two major errors. A temperature error due to combustion, endothermic decomposition, thermal gradients, or thermocouple error approached a maximum of $\pm$10°C. Weight error was largely due to electrical component drift plus a pressure change effect for vacuum runs. The drift and pressure errors ranged up to maximum values of about 0.75 and 3.25% weight loss at 950°C, respectively.

SECTION XI

CONCLUSIONS AND RECOMMENDATIONS

Constant heating rate thermogravimetry in oxidizing atmospheres was a rapid and useful method for studying sample and environmental variables empirically, verifying mechanisms, and estimating Arrhenius constants from constant surface area data. The potential ease of shifting major sample and environmental variables over wide ranges with corresponding shifts in apparent surface reaction control effects or diffusion control effects was attractive for studying phase boundary control or other oxidative mechanisms. Isothermal thermogravimetry was more promising for defining exact mechanisms and evaluating Arrhenius constants precisely.

There were problem areas in the precise use of either constant heating rate or isothermal thermogravimetry. Approaches for (1) holding critical variables at a constant level during the run, and (2) reducing experimental error included:

1. Heating rate - accurate heating rate based upon sample temperature.

2. Isothermal temperature - sample temperatures consistent with rapid weight loss and zero thermal inertia for the sample.

3. Oxygen concentration - a miniature sample immersed within a constant velocity, high mass flow, preheated stream of oxidizing gas.

4. Pressure - a manostat or other device for pressure control.

5. Pretreatment - sample pretreatments to assess effects.

6. Surface area - a carefully designed, near constant area sample.

7. Temperature error - a miniature sample/holder with direct sample thermocouple emplacement.

8. Weight error - a miniature sample/holder and pressure control.

9. Density, porosity, pore spectra, and specific surface area - interrupted thermogravimetry runs to assess constancy.

The recording thermobalance was extensively modified for the thermogravimetry of ablative plastics to 1400°C in helium purging flow. Although there were no further oxidative experiments, several new and planned features were amenable to solving identified problem areas (Reference 30). These included, for example, a wide range of heating rates, little thermal inertia for isothermal runs over a wide temperature range, a high velocity gas purge around a carefully designed sample, a vacuum/purge gas network, a potential variety of solid sample configurations, direct thermocouple instrumentation of the sample, reduced experimental error, and easy interruption of the run at anytime.

APPENDIX

TRIM EMPIRICAL KINETICS COMPUTER CODE

TRIM was a general computer code for empirical kinetics (References 19 and 20). Arrhenius constants were calculated from integral weight fractions as a function of temperature for a constant heating rate. Many data points were therefore possible without the chore of often inaccurate weight loss rate measurements.

The general kinetic model of surface reaction oxidation was

$$-dw/dT = (B/\dot{T})\, e^{-X}$$

For this model, TRIM solved

$$\log_{10}((1 - w)/T^{2}) = -(E/R \ln 10)(1/T) + \log_{10} r(BR/E\dot{T})$$

The terms $-(E/R \ln 10)$ and $\log_{10} r(BR/E\dot{T})$ were made equal to a slope and an intercept, respectively, for this nearly linear equation. E and the product rB were estimated by the standard method of least squares. Knowing E, an "averaged" value of the near constant r could be estimated by either (1) direct calculation using Equation 12 or (2) as a reference in a table (or figure) as a function of X. Knowing r, B followed from the product rB.

PAR 3 was a useful companion to TRIM. This computer code graphically constructed a thermogram from input kinetic constants. For the present model, PAR 3 solved Equation 8 for a given number of weight/temperature

data points. The results would be plotted graphically by an X-Y plotter in the standard thermogram format. PAR 3 was a potentially useful means of assessing the relative importance of B and component terms.

REFERENCES

1. L. Kaufman and H. Nesor. Stability Characterization of Refractory Materials Under High Velocity Atmospheric Flight Conditions, Part I, Volume I: Summary. AFML-TR-69-84, Part I, Volume I, And Parts I-IV thereto. Air Force Materials Laboratory, Wright-Patterson Air Force Base, Ohio. December 1969.

2. S. Scala. The Ablation of Graphite in Dissociated Air. I. Theory. R62SD72. General Electric Company. September 1962. Also presented at the IAS National Summer Meeting, Los Angeles, California. 19-22 June 1962.

3. R. Price and F. Schultz. Modification of the One-Dimensional REKAP Program to Allow for Charring in Three Material Layers. NASA CR-72488. January 1969.

4. J. Baron and H. Bernstein. "Heterogeneous Rate Coupling for Graphite Oxidation." AIAA 5th Thermophysics Conference, Los Angeles, California. 29 June-1 July 1970. AIAA Paper No. 70-823.

5. R. Kendall and E. Bartlett. Non-Similar Solution of the Multi-component Laminar Boundary Layer by an Integral Matrix Method. Report 66-7, Part III. Aerotherm Corporation, Mountain View, California. 1967.

6. M. Levy and P. Wong. Oxidation of Several Commercial-Grade Graphites at Elevated Temperatures. WAL-TR-852. 4/2 Watertown Arsenal, Watertown, Massachusetts. November 1962.

7. N. Diaconis, T. Shaw, and W. Warren, Jr. The Hypervelocity Heat Protection Program. R65SD60. General Electric Company.

8. R. Tanzilli. Evaluation of Graphite Composites in Re-Entry Environments. AFML-TR-65-328. Air Force Materials Laboratory, Wright-Patterson Air Force Base, Ohio. October 1965.

9. D. Sallis, et al. Evaluation of Ablative Materials. AFML-TR-66-348, Volume III. Air Force Materials Laboratory, Wright-Patterson Air Force Base, Ohio. September 1967.

10. [illegible] Bartlett. Analytical and Graphical Prediction of Graphite Ablation Rates and Surface Temperatures During Re-Entry at 25,000 to 45,000 Feet per Second. FTC-TDR-63-40. Air Force Flight Test Center, Edwards Air Force Base, California. March 1964.

11. Private communication. J. Cresswell, General Electric Company.

12. R. Carlson, et al. Carbonized Plastic Composites for Hyperthermal Environments. ASD-TDR-62-352, Air Force Materials Laboratory, Wright-Patterson Air Force Base, Ohio. June 1962.

REFERENCES (CONTINUE)

13. R. Farmer. Thermogravimetry of Phenol-Formaldehyde Polycondensates. AFML-TR-65-246. Air Force Materials Laboratory, Wright-Patterson Air Force Base, Ohio. January 1966.

14. W. Gilwee and A. Sporzynski. Plastic Composites. TM-4076. TRW Equipment Laboratories, Cleveland, Ohio. 31 March 1965.

15. R. Farmer. Thermal Analysis of Ablative Plastic Materials. Part I. Constant Heating Rate Thermogravimetry of Carbon/Graphite Cloth Reinforced Aromatic/Heterocyclic Resins to 1400°C. AFML-TR-70-35. Air Force Materials Laboratory, Wright-Patterson Air Force Base, Ohio. August 1970.

16. S. Scala. "The Hypersonic Ablation of Graphite." Chapter 16. Developments in Heat Transfer. W. Rohsenow, Ed.

17. M. Levy and A. Tarpinian. Oxidation Resistance of Some Commercial Grade Graphites. WAL-TR-825. 4/1. Watertown Arsenal, Watertown, Massachusetts. May 1959.

18. M. Levy. Oxidation of Pyrolytic Graphite Between 1250F and 1850F. WAL-TR-851. 4/1. Watertown Arsenal, Watertown, Massachusetts. May 1961.

19. R. Farmer. Thermogravimetry of Phenol-Formaldehyde Polycondensates Part II. Empirical Kinetic Parameters. AFML-TR-65-246, Part II. Air Force Materials Laboratory, Wright-Patterson Air Force Base, Ohio. March 1967.

20. N. Olson. A Computer Method for the Thermogravimetry of Ablative Plastic Materials. Empirical Kinetics and Thermogram Construction AFML-TR-70-262. Air Force Materials Laboratory, Wright-Patterson Air Force Base, Ohio. October 1970.

21. M. Levy. Surface Area Effects on the Oxidation Kinetics of Pyrolytic Graphite. AMRA-TR-67-20. US Army Materials Research Agency, Watertown, Massachusetts. June 1967.

22. M. Levy. "Surface Area Effects and the Oxidation Kinetics of Pyrolytic Graphite." Paper in Thermal Analysis. Volume 2. Inorganic Materials and Physical Chemistry. Academic Press, New York, 1969.

23. G. Blyholder and H. Eyring. Kinetics of Graphite Oxidation. AFOSR-TN-56-451. 15 August 1956.

24. G. Blyholder and H. Eyring. "Kinetics of Graphite Oxidation." J. Phy. Chem. 61, 682(1957).

REFERENCES (CONTINUE)

25. E. Gulbransen, et al. "The Oxidation of Graphite at Temperatures at 600 to 1500C, and at Pressures of 2 to 76 Torr of Oxygen." J. Ele. Soc. 110 (June 1963).

26. J. Ong, Jr. "On the Kinetics of Oxidation of Graphite." Int. J. of Carbon 2, 281 (1964).

27. H. Schwartz, et al. Properties of Thermally Degraded Ablative Plastics. WADD-TN-60-286. Air Force Materials Laboratory, Wright-Patterson Air Force Base, Ohio. January 1961.

28. National Industrial Carbon and Graphite Products. National Carbon Company, Division of Union Carbide Corporation. 1957.

29. F. Nelson and F. Eggertsen. "Determination of Surface Area Absorption Measurements by a Continuous Flow Method." Ana. Chem. 30, 1387 (1958).

30. R. Farmer. Thermal Analysis of Ablative Plastic Materials. Part II. Kinetics and Physicochemical Mechanisms for the Ablation of Phenolic Resin Materials. AFML-TR-70-35. Air Force Materials Laboratory, Wright-Patterson Air Force Base, Ohio (to be published).

UNCLASSIFIED
Security Classification

DOCUMENT CONTROL DATA - R & D

(Security classification of title, body of abstract and indexing annotation must be entered when the overall report is classified)

1 ORIGINATING ACTIVITY (Corporate author)	2a. REPORT SECURITY CLASSIFICATION
Air Force Materials Laboratory Wright-Patterson AFB, Ohio 45433	UNCLASSIFIED 2b GROUP

3 REPORT TITLE

THE MODELING OF THERMOCHEMICAL ABLATION OF PYROLYZED PLASTICS AND GRAPHITES, PART I. APPLICATIONS OF OXIDATIVE THERMOGRAVIMETRY TO EVALUATING ARRHENIUS CONSTANTS AND DEFINING MECHANISMS

4 DESCRIPTIVE NOTES (Type of report and inclusive dates)

5 AUTHOR(S) (First name, middle initial, last name)

Farmer, R. W.

6 REPORT DATE	7a. TOTAL NO OF PAGES	7b. NO OF REFS
FEBRUARY 1972		30

8a. CONTRACT OR GRANT NO	9a. ORIGINATOR'S REPORT NUMBER(S)
b. PROJECT NO 7340	AFML-TR-71-207
c. Task No. 734001	9b. OTHER REPORT NO(S) (Any other numbers that may be assigned this report)
d.	

10 DISTRIBUTION STATEMENT Distribution limited to U.S. Government agencies only; test and evaluation; statement applied September 1971. Other requests for this document must be referred to the Plastics and Composites Branch (AFML/LNC), Nonmetallic Materials Division, Air Force Materials Laboratory, Wright-Patterson AFB, Ohio 45433.

11 SUPPLEMENTARY NOTES	12 SPONSORING MILITARY ACTIVITY
	Air Force Materials Laboratory/LNC Wright-Patterson AFB, Ohio 45433

13 ABSTRACT

Future reentry vehicles will use pyrolyzed plastics and monolithic graphites for shape stable, thermal protection systems. Oxidation kinetic models and kinetic constants for these models will be necessary to predict (1) linear and mass losses, (2) altered heat and mass transport features of the ablation contaminated flow field, (3) the effects of ablative and contaminant species on optical/radar observables, and (4) related phenomena.

Constant heating rate thermogravimetry was used to study the fundamental kinetics and mechanisms of surface oxidation at temperatures to 1000°C. The materials included an ablative pyrolyzed plastic, an ammonium chloride-filled version of this material, three graphites, graphite fabric, and a carbon.

The thermograms of powder samples of the pyrolyzed plastic and most of the other materials were similar. Oxidative resistance was reduced by an increase in airflow rate, heating rate, oxygen concentration, pressure, or surface area. These sample and environmental responses were consistent with an Arrhenius-type kinetic model.

There was evidence of diffusive effects, of the type normally found at temperatures above 1000°C, in some of the heating rate, oxygen concentration, and surface area experiments. This unexpected result was tentatively explained in terms of a phase boundary control theory of surface oxidation.

The recording thermobalance was unsatisfactory in operation over a sufficiently wide range of sample and environmental variables for a comprehensive investigation of kinetics and mechanisms. A prototype version of a unique gas purge/vacuum network was therefore built and demonstrated over an extremely wide range of environmental variables

DD FORM 1 NOV 65 1473

UNCLASSIFIED
Security Classification

14 KEY WORDS	LINK A		LINK B		LINK C	
	ROLE	WT	ROLE	WT	ROLE	WT
Ablation						
Ablative Materials						
Carbon						
Graphite						
Kinetics						
Kinetics And Mechanisms						
Oxidation						
Pyrolyzed Plastics						

U.S. Government Printing Office: 1972 — 759-066/578